DOI: 10.1534/genetics.109.103614

The Cation Diffusion Facilitator Gene *cdf-2* Mediates Zinc Metabolism in *Caenorhabditis elegans*

Diana E. Davis,* Hyun Cheol Roh,* Krupa Deshmukh,* Janelle J. Bruinsma,*,[1] Daniel L. Schneider,* James Guthrie,[†] J. David Robertson[‡] and Kerry Kornfeld*,[2]

**Department of Developmental Biology, Washington University School of Medicine, Saint Louis, Missouri 63110,* [†]*Research Reactor Center and* [‡]*Department of Chemistry, University of Missouri, Columbia, Missouri 65211*

Manuscript received April 6, 2009
Accepted for publication May 12, 2009

ABSTRACT

Zinc is essential for many cellular processes. To use *Caenorhabditis elegans* to study zinc metabolism, we developed culture conditions allowing full control of dietary zinc and methods to measure zinc content of animals. Dietary zinc dramatically affected growth and zinc content; wild-type worms survived from 7 μM to 1.3 mM dietary zinc, and zinc content varied 27-fold. We investigated *cdf-2*, which encodes a predicted zinc transporter in the cation diffusion facilitator family. *cdf-2* mRNA levels were increased by high dietary zinc, suggesting *cdf-2* promotes zinc homeostasis. CDF-2 protein was expressed in intestinal cells and localized to cytosolic vesicles. A *cdf-2* loss-of-function mutant displayed impaired growth and reduced zinc content, indicating that CDF-2 stores zinc by transport into the lumen of vesicles. The relationships between three *cdf* genes, *cdf-1*, *cdf-2*, and *sur-7*, were analyzed in double and triple mutant animals. A *cdf-1* mutant displayed increased zinc content, whereas a *cdf-1 cdf-2* double mutant had intermediate zinc content, suggesting *cdf-1* and *cdf-2* have antagonistic functions. These studies advance *C. elegans* as a model of zinc metabolism and identify *cdf-2* as a new gene that has a critical role in zinc storage.

ZINC plays many roles in biological systems, including binding to proteins and promoting specific conformations, such as the zinc finger, and contributing to the active site of enzymes (Vallee and Falchuk 1993). Reflecting its multiple uses, organisms that do not obtain adequate dietary zinc display a wide range of defects (Cole *et al.* 1999; Kambe *et al.* 2004; Chowanadisai *et al.* 2005; Herbig *et al.* 2005; Dufner-Beattie *et al.* 2007). For example, humans that are zinc deficient have abnormalities of multiple systems including the skin and immune system (Hambidge 2000; Chowanadisai *et al.* 2006; Hambidge and Krebs 2007; Maverakis *et al.* 2007). Excess dietary zinc can also cause defects as a result of zinc toxicity (Koh *et al.* 1996; Nies 2007). The mechanisms underlying zinc toxicity have not been clearly defined but may involve the substitution of zinc for other metals such as copper (Zhao and Eide 1997). Animals have evolved sophisticated mechanisms to regulate zinc metabolism to ensure an adequate supply of zinc but avoid zinc toxicity. Zinc metabolism involves uptake of zinc from dietary sources into intestinal cells, distribution of zinc throughout the body to supply nonintestinal cells, insertion of zinc into zinc-requiring proteins, and excretion of excess zinc from cells and the animal. An essential aspect of zinc metabolism is adapting to changing levels of dietary zinc. Homeostasis is likely to involve sensors that monitor available zinc and effector mechanisms that adjust intake, storage, and excretion of zinc (Tapiero and Tew 2003). These important processes are not well characterized.

Zinc in biological systems is the Zn^{2+} ion, and Zn^{2+} does not diffuse across lipid bilayers (Stryer 1995). In metazoans, two families of transmembrane proteins play critical roles in transporting zinc, the cation diffusion facilitator (CDF/SLC30) family (Palmiter and Huang 2004) and the Zrt-, Irt- like protein (ZIP/SLC39) family (Eng *et al.* 1998; Guerinot 2000; Eide 2004). The CDF family evolved in prokaryotes and has been conserved in fungi, plants, and animals. Yeast contain multiple CDF proteins, which are localized to specific membrane compartments (Eide 2006). Vertebrates contain 10 predicted CDF proteins (Liuzzi and Cousins 2004; Palmiter and Huang 2004; Seve *et al.* 2004). Mutations in human ZnT-2 are implicated in diseases characterized by inadequate zinc in breast milk, suggesting that CDF proteins play essential roles in zinc metabolism in humans (Chowanadisai *et al.* 2006). Most CDF proteins are predicted to contain six transmembrane regions, and the N and C termini are predicted to be

Supporting information is available online at http://www.genetics.org/cgi/content/full/genetics.109.103614/DC1.

[1]*Present address:* EMD Chemicals, Madison, WI 53719.

[2]*Corresponding author:* Department of Developmental Biology Washington University School of Medicine, Box 8103, 660 South Euclid Ave., St. Louis, MO 63110. E-mail: kornfeld@wustl.edu

cytoplasmic. Recent crystallographic data suggest that the *Escherichia coli* CDF protein YiiP functions as a dimer (Lu and Fu 2007), consistent with the results of cell biology studies in yeast (Ellis *et al.* 2005). The energy source for CDF proteins appears to be ion gradients, such as H^+ and K^+ (Guffanti *et al.* 2002; Chao and Fu 2004).

Given that animals contain multiple CDF proteins, a critical question is: How do these proteins function in a coordinated manner to mediate zinc metabolism throughout the animal? One mechanism is cell-type-specific expression. For example, vertebrate ZnT-3 is expressed primarily in neuronal cells, where it promotes zinc accumulation in synaptic vesicles (Palmiter *et al.* 1996b; Cole *et al.* 1999). A second mechanism is localization to specific membrane compartments. For example, vertebrate ZnT-8 is localized to insulin granules (Chimienti *et al.* 2004), whereas vertebrate ZnT-1 is localized to the plasma membrane (Palmiter and Findley 1995). A third mechanism is intrinsic differences in activity, which might include differences in affinity for zinc (K_M), differences in the rate of zinc transport (V_{max}), and differences in metal specificity. A fourth mechanism is differences in regulation that adjust protein abundance and activity in response to fluctuating dietary zinc, which might include transcriptional, post-transcriptional, and post-translational regulation. These mechanisms are not mutually exclusive, and additional mechanisms may also be utilized. An understanding of how multiple CDF proteins function coordinately in an animal will require a genetically tractable model system that can be used to dissect the complementary, redundant, and antagonistic activities of multiple CDF proteins.

The nematode *Caenorhabditis elegans* has been a powerful model system to study many biological processes, but studies of nutrient biology have been limited. The use of *C. elegans* to study metal biology has included analyses of heme, magnesium, zinc, and cadmium (Bruinsma *et al.* 2002; Bruinsma *et al.* 2008; Dong *et al.* 2008a; Rajagopal *et al.* 2008; Kemp *et al.* 2009). The fully sequenced *C. elegans* genome contains 14 predicted genes that encode CDF proteins (Kambe *et al.* 2004; K. Deshmukh and K. Kornfeld, unpublished observation). Two of these genes have been analyzed genetically, *cdf-1* and *sur-7* (Bruinsma *et al.* 2002; Yoder *et al.* 2004). Loss-of-function mutations of *cdf-1* and *sur-7* were identified in forward genetic screens for modifiers of abnormal vulval cell fates caused by constitutively activated Ras. In addition to promoting Ras-mediated signal transduction, *cdf-1* and *sur-7* promote survival in high dietary zinc, since loss-of-function mutations of these genes cause sensitivity to high dietary zinc (Bruinsma *et al.* 2002; Yoder *et al.* 2004). *cdf-1* is expressed in intestinal cells and vulval cells, and CDF-1 protein is localized to the plasma membrane (Bruinsma *et al.* 2002). *sur-7* is expressed in nonintestinal cells, and SUR-7 protein is diffusely localized to the cytosol, suggesting it is localized to an internal membrane (Yoder *et al.* 2004). The functions of the remaining predicted *cdf* genes in *C. elegans* have not been determined.

To use *C. elegans* as a model system to study zinc metabolism and CDF protein function, we developed culture conditions that allow full control of dietary zinc. Here we show that worms are sensitive to both low and high dietary zinc and that sensitivity to dietary zinc can be used to assay zinc metabolism. We developed methods to measure the zinc content of *C. elegans* and demonstrated that dietary zinc strongly influences zinc content of wild-type animals. These methods advance the utility of *C. elegans* as a model system to study zinc metabolism. We investigated the function of a new predicted *cdf* gene, which we named *cdf-2*. CDF-2 is most similar to vertebrate ZnT-2, which is localized to vesicles and implicated in human diseases of zinc deficiency (Chowanadisai *et al.* 2006). The *cdf-2* transcript abundance was increased at high levels of dietary zinc, suggesting that *cdf-2* is involved in zinc homeostasis. CDF-2 protein was expressed in intestinal cells and localized to cytosolic vesicles. A strong loss-of-function mutation of *cdf-2* was characterized; mutant animals displayed growth defects and reduced zinc content compared to wild-type animals, indicating that *cdf-2* functions in zinc storage. To explore the relationship between the functions of multiple *cdf* genes, we analyzed double and triple mutant animals with mutations in *cdf-1*, *cdf-2*, and *sur-7*. The results indicate that *cdf-1* and *cdf-2* have antagonistic functions in mediating zinc content and *cdf-2* plays an important role in zinc storage by sequestering zinc in the lumen of cytosolic vesicles.

MATERIALS AND METHODS

General methods and strains: *C. elegans* were cultured at 20° on nematode growth medium (NGM) dishes with live *E. coli* as described by Brenner (1974) or in *C. elegans* maintenance medium (CeMM, described below) (Szewczyk *et al.* 2003). The wild-type strain and parent of all mutant strains was Bristol N2. The following mutations were used: *unc-119(ed3 R113Stop)* is a loss-of-function mutation that causes a strong uncoordinated phenotype and an inability to form dauer larvae (Maduro and Pilgrim 1995). *let-60(n1046 G13E)* is a semidominant, gain-of-function allele of the Ras gene (Beitel *et al.* 1990). *cdf-1(n2527 Q156Stop)* is a strong loss-of-function allele caused by a nonsense change in exon 4 (Bruinsma *et al.* 2002). *sur-7(ku119)* is a partial loss-of-function allele caused by a single nucleotide change near the splice donor of exon 3 (Yoder *et al.* 2004). *cdf-2(tm788)* has an 804-bp deletion with a 68-bp insertion that removes the first 34 codons and is likely to cause a strong loss of function (described here). *cdf-1*, *cdf-2*, and *sur-7* are located on chromosome X, and we generated *cdf-1 cdf-2*, *cdf-1 sur-7*, and *cdf-2 sur-7* double mutant animals using standard techniques and confirmed the genotypes by PCR and gel electrophoresis (*cdf-2*) and DNA pyrosequencing (*cdf-1* and *sur-7*; PSQ 96 MA, Biotage, Charlottesville, VA). A *cdf-1 cdf-2 sur-7* triple mutant was generated from *cdf-1 cdf-2* and *cdf-2 sur-7* double mutant animals using standard techniques.

Preparation of CeMM and culturing worms in CeMM: A solution of 2× CeMM was prepared as described by Szewczyk *et al.* (2003) with minor modifications. Briefly, we prepared five solutions (amino acids, nucleic acids, water-soluble growth factors and vitamins, triethanolamine-soluble growth factors and vitamins, and trace metal salts without zinc chloride), combined these to yield 2× CeMM with no added zinc, adjusted the pH to 5.9 with 10% (w/v) NaOH, filtered the medium through a 0.22-μm cellulose acetate filter (Corning Life Sciences, Lowell, MA), and stored the medium in the dark at 4° for up to 8 months. To use the CeMM, we diluted with water from a Milli-Q Synthesis A10 machine (Millipore, Billerica, MA) to yield 1× CeMM. To achieve the final zinc concentration of 1× CeMM, we added the appropriate volume of 1 mm, 10 mm, 100 mm, or 1 m zinc chloride (Z0152, Sigma-Aldrich, St. Louis) diluted in 40 mm HCl. To equalize the amount of HCl diluent added to each medium sample, we added the appropriate volume of 40 mm HCl with no added zinc. The 1× CeMM with added zinc was used promptly and not stored.

To introduce worms that were growing on NGM with live *E. coli* into CeMM, we collected adults and treated the animals with NaOH and bleach to generate eggs free of bacterial contamination (Wood 1988). Subsequent procedures were performed in a tissue culture hood using sterile technique. Eggs were transferred to 25 cm^2 T-flasks (TPP, Trasadingen, Switzerland) containing 5 ml M9 buffer (85 mm NaCl, 22 mm KH_2PO_4, 42 mm Na_2HPO_4, 1 mm $MgSO_4$) and 10 μl/ml antibiotic-antimycotic solution (10,000 units penicillin, 10 mg streptomycin, and 25 μg amphotericin B/ml, Sigma-Aldrich). Eggs were cultured at 20° for 2–3 days to allow the hatching and developmental arrest of L1 larvae. Larvae were washed two times in M9 buffer, transferred to a 25 cm^2 T-flask in 5 ml CeMM containing 30 μm zinc chloride, and cultured at 20° with no agitation for 3–4 weeks until visual inspection revealed significant growth of the population. Worms were collected using Pasteur pipets, pelleted by centrifugation at 1000 rpm for 5 min at 15°, washed two times in M9 buffer, resuspended in 15 ml CeMM containing 30 μm zinc chloride and transferred to 75 cm^2 T-flasks (TPP).

Maturity analysis: Worms were grown on NGM with live *E. coli* and treated with NaOH and bleach to collect eggs. For experiments scored with a dissecting microscope, eggs were diluted in CeMM (19 zinc concentrations), seeded in 24-well plates (TPP) at a concentration of 100 eggs in 500 μl, and incubated at 20° in a box containing moist paper towels to increase humidity. After 9 days, animals were collected, examined using a dissecting microscope, and scored as larval (<1 mm and larval morphology) or adult (>1 mm and adult morphology). For experiments using the COPAS Biosort (Union Biometrica, Holliston, MA), eggs were added to 5 ml M9 buffer containing 10 μl/ml antibiotic-antimycotic solution (Sigma-Aldrich) and incubated for 2–3 days at 20°. Resulting L1 larvae were diluted in CeMM (18 zinc concentrations), seeded in 24-well plates at a concentration of 100 L1 larvae in 500 μl, and incubated at 20° in a box containing moist paper towels. After 12 days, animals were transferred to 96-well plates and analyzed using the ReFLx Sampler of a COPAS Biosort.

Population growth rate analysis: To prepare 15–16 cultures for a comparative analysis, we generated a large population of worms growing in CeMM containing 30–75 μm zinc chloride. We counted an aliquot to determine the number of worms in the sample, collected the worms by centrifugation, washed two times in M9 buffer, and resuspended at 10,000 worms/ml in CeMM with no added zinc. For cultures scored using a dissecting microscope, 2.5 ml of worms were transferred to a 25 cm^2 T-flask containing 2.5 ml of CeMM with added zinc to generate final zinc concentrations that ranged from 0 to 2 mm. For cultures scored using the COPAS Biosort, 7.5 ml of worms were transferred to a 75 cm^2 T-flask containing 7.5 ml of CeMM with added zinc to generate final zinc concentrations that ranged from 0 to 2.5 mm. In both cases, the initial worm concentration was 5000 worms/ml. The cultures were incubated at 20° for up to 22 days. To determine the number of worms in the sample using a dissecting microscope, we removed 100 μl of the culture, diluted the sample with M9 buffer containing 0.01% Triton X-100 to yield an approximate worm concentration of 1 worm/μl, spotted 100 μl onto an NGM dish, and counted the number of larvae and adults. Each sample was scored three times. To determine the number of worms in the sample using the COPAS Biosort, we employed 45-μm fluorescent beads (Fluoresbrite beads, Poly Sciences, Warrington, PA) as a counting standard. Beads were diluted to a concentration of ~20 beads/μl. We combined a known number of beads with a sample of worms in ~8 ml M9 buffer with 0.01% Triton X-100, used the COPAS Biosort to count the number of beads and the number of worms, calculated the ratio of worms to beads, and then calculated the concentration of worms in the initial culture. The use of the fluorescent beads allowed us to determine the total number of worms in an aliquot even though not all of the aliquot flowed past the detector. To determine the population growth rate, we plotted the number of worms per milliliter *vs.* the number of days in culture and performed a linear regression analysis using Microsoft Excel (Microsoft, Redmond, WA). The linear portion of the plot was from day 7 to day 17 (Figure 2B and data not shown), and we defined this slope as the population growth rate. To determine the population growth rates that were half the maximal population growth rate (EC_{50} and IC_{50}), we analyzed the 16 population growth rates determined during a single growth trial using GraphPad Prism 5.0 (GraphPad Software, La Jolla, CA). The EC_{50} and IC_{50} were determined from the population growth rates at dietary zinc concentrations from 1 μm to 120 μm and 60 μm to 2.5 mm, respectively, by fitting these data to a dose–response curve with the bottom constrained to zero and a variable Hill slope. Two to three independent EC_{50} and IC_{50} values were determined for each strain, and the average, standard deviation, and *P*-values were calculated using Microsoft Excel.

Determination of zinc content of *C. elegans* using radioactive ^{65}Zn: $^{65}ZnCl_2$ was purchased from Perkin Elmer (Waltham, MA), and the initial specific activity varied from ~1 to 3 μCi/μg. To culture worms with ^{65}Zn, we determined the concentration of worms in a large starting culture, pelleted the worms, washed the worms two times in M9 buffer, resuspended the worms in CeMM with no added zinc, dispensed 30,000 worms in 300 μl into 24-well plates, and added 300 μl of CeMM with added zinc to yield final zinc concentrations of 6 μm, 10 μm, 30 μm, 75 μm, 350 μm, 1 mm, and 2 mm. To generate CeMM with zinc concentrations of 6 μm, 10 μm, and 30 μm, we used undiluted $^{65}ZnCl_2$ with a specific activity of ~1μCi/μg. To generate CeMM with zinc concentrations of 75 μm, 350 μm, 1 mm, and 2 mm, we combined $^{65}ZnCl_2$ (~1μCi/μg) with nonradioactive $ZnCl_2$ to yield samples where the specific activity of the ^{65}Zn was reduced by the dilution factors 2.5, 11, 33, and 67, respectively. Samples were incubated at 20° for 12–15 days. To minimize evaporative loss, we placed samples in plastic bags with moist paper towels. Worms were collected in a 0.2-μm Nanosep MF filtration device (Pall Scientific, East Hills, NY) by centrifugation and washed two times in M9 with 100 mm EDTA to chelate unincorporated zinc. To eliminate ^{65}Zn in the intestinal lumen, we incubated the worms for 30 min in CeMM with the corresponding unlabeled zinc concentration and 1 mm serotonin (Sigma-Aldrich) to stimulate pharyngeal pumping and defecation (Horvitz *et al.* 1982). Thirty minutes was sufficient time for worms to expel

^{65}Zn from the intestinal lumen (data not shown). Worms were collected in a 0.2-μm Nanosep filtration device by centrifugation and washed two times in M9 with 100 mM EDTA. Serial dilutions of $^{65}ZnCl_2$ were measured with a Beckman gamma 4000 (Beckman Coulter, Fullerton, CA) to generate a standard curve that was used to determine the amount of ^{65}Zn in each worm sample. The samples were stored at −80°. To determine the amount of protein in each worm sample, we added 100 mM NaCl containing Complete Mini Protease Inhibitor Cocktail tablets (Roche, Basel, Switzerland) to each sample, sonicated to disrupt the cuticle using a Digital Sonifer 450-D (Branson Ultrasonics Corporation, Danbury, CT), and determined the amount of protein using the Micro BCA Protein Assay Reagent kit (Pierce, Rockford, IL) according to the manufacturer's instructions. The zinc content of worms (ng zinc/μg protein) was calculated using the formula [^{65}Zn (μCi)/sample ÷ specific activity (μCi/μg) × 1000 ng/μg] ÷ [protein (μg)/volume × volume/sample].

Determination of zinc content of *C. elegans* using inductively coupled plasma-mass spectrometry: A large population of worms growing in CeMM containing 30 μM zinc chloride was generated to initiate seven cultures for a comparative analysis. We determined the number of worms in the sample, collected the worms by centrifugation, and washed the worms two times in M9 buffer. The worms were resuspended at 20,000 worms/ml in CeMM with no added zinc, and 7.5 ml of worm solution were transferred to a 75-cm^2 T-flask containing 7.5 ml of CeMM with added zinc to yield the zinc concentrations 6 μM, 10 μM, 30 μM, 75 μM, 350 μM, 1 mM, and 2 mM, and an initial worm concentration of 10,000 worms/ml. Samples were cultured at 20° for 16–18 days. Worms were collected by centrifugation and washed two times in M9 buffer. To eliminate zinc in the intestinal lumen, we incubated the worms for 30 min in M9 buffer with 1 mM serotonin. Worms were washed two times in M9 buffer, transferred to precleaned and preweighed 15-ml polypropylene tubes (Stockwell Scientific, Scottsdale, AZ) and frozen at −80°. The metal content of the sample was determined using inductively coupled plasma-mass spectrometry (ICP-MS) as described by Dong *et al.* (2008b). Briefly, the sample was desiccated, weighed, digested with concentrated nitric acid and hydrogen peroxide solution (HNO_3, Fisher OPTIMA Grade, Thermo Fisher Scientific, Wilmington, DE; 30% H_2O_2, Fluka *Trace*SELECT Ultra, Sigma-Aldrich) in an ultrasonic bath at 60° for 1 hr, diluted with ultra-pure 18.2 MΩ·cm deionized water, reweighed, mixed by repeated inversion, and diluted with 2% HNO_3 in H_2O. Empty tubes were processed identically to the samples as a control. An internal standard was added to each sample and control to correct for matrix effects in the instrument. Weights were recorded at each step so that exact gravimetric dilution factors could be calculated for all samples and controls. The copper, iron, manganese, and zinc content of each sample and control was determined using a VG Axiom high-resolution ICP-MS (Thermo Fisher Scientific). Instrument calibration standards were prepared by diluting ICP-MS multielement calibration standards (High-Purity Standards, Charleston, SC), which are manufactured following National Institute of Standards and Technology Standard Reference Materials procedures. The instrument limit of detection (LOD) was calculated as 3× the standard deviation of the concentration of a given analyte measured in 10 runs of a zero point standard (2% HNO_3 solution with internal standard). The sample LOD was calculated by multiplying the instrument LOD by the total sample dilution factor. The metal content of the worms was calculated using the following formula: [zinc/sample ÷ sample weight].

One consideration with using CeMM is the possibility that worm metabolism during the culture period significantly changes the medium composition. Szewczyk *et al.* (2003) monitored pH during a 2-week incubation and demonstrated that the starting pH of 6 gradually increases to about 7. We confirmed these results and observed that after ~25 days in culture the pH begins to increase significantly; therefore, worms were not cultured for >22 days. To monitor changes in media zinc concentrations, we used radioactive ^{65}Zn to determine the fraction of total zinc incorporated into worms in 109 independent samples with zinc concentrations ranging from 6 μM to 2 mM and initial worm concentrations of 50 worms/μl. The fraction of total zinc incorporated into worms that were cultured for 12–15 days varied from 0.02 to 2.4%. There was a trend toward lower fractional zinc incorporation as the dietary zinc concentration increased. These results indicate that worm metabolism has a minimal effect on the concentration of dietary zinc in the medium during the course of these experiments.

Analysis of *cdf-2* transcripts: RNA was isolated from wild-type animals cultured on NGM dishes with live *E. coli*. Mixed-staged animals were collected, washed in M9 buffer, and solubilized in TRIzol (Invitrogen, Carlsbad, CA). The RNA concentration and quality was determined using a NanoDrop 100 (Thermo Fisher Scientific). cDNA was generated using the SuperScript III First-Strand Synthesis System for RT–PCR (Invitrogen) using either an oligo(dT) primer or random hexamer oligonucleotide primers. PCR and DNA sequencing were performed according to standard methods. Primers annealing in exon 1 and exon 8 amplified the expected 959-bp product and did not amplify any shorter products, suggesting that any alternatively spliced transcripts are of low abundance. A primer annealing in exon 7 and an oligo(dT) primer amplified an ~425-bp product. DNA sequencing demonstrated an ~30-bp adenosine tract immediately following the sequence ACAGC, indicating the addition of a polyadenosine tail 120 bp downstream of the stop codon.

Quantitative, real-time PCR analysis: To generate cultures for a comparative analysis, we began by generating a large population of worms growing in CeMM containing 30 μM zinc chloride. Worms were collected by centrifugation, washed two times in M9 buffer, resuspended in CeMM with 2 μM, 10 μM, 30 μM, 250 μM, 500 μM, 1 mM, or 2 mM zinc chloride, transferred to 25 cm^2 T-flasks, and incubated at 20° for 6 days. To collect a synchronous population of adult worms, we diluted the culture in 50 mM Tris HCl, pH 6.4 containing 2 μM, 10 μM, 30 μM, 250 μM, 500 μM, 1 mM, or 2 mM zinc chloride, respectively, and used the COPAS Biosort to select 1000 adults from a mixed-stage population. RNA was purified using TRIzol, resuspended at a concentration of ~250 ng/μl, and treated with DNase I (Turbo DNA Free kit, Applied Biosystems, Foster City, CA). cDNA was synthesized using the High-Capacity cDNA Reverse Transcription kit from Applied Biosystems according to the manufacturer's instruction using random hexamer oligonucleotide primers. Quantitative, real-time PCR was performed using a BioRad MyiQ Single Color Real-Time PCR Detection System thermocycler and iQ SYBR Green Supermix (BioRad Laboratories, Hercules, CA). Forward and reverse amplification primers were: *ama-1*, atcggag cagccaggaactt and ggactgtatgatggtgaagctgg; *cdf-1*, gcattaaa atcgctactcgcc and ccgtacacataaagattccgttg; *cdf-2*, atagcaatcgga gagcaacg and tgtgacaattgcgagtgagc; *rps-23*, aaggctcacattggaa ctcg and aggctgcttagcttcgacac; and *sur-7*, ctttatcgaaccgctgga ac and cgagtgggtcgctgaattg. The amplified products were confirmed by DNA sequencing. The efficiency (*E*) of each primer pair was determined using cDNA from mixed-stage worms as template. The average primer pair efficiency was calculated from three independent experiments and ranged from 87 to 109%. To calculate the change in transcript abundance between two conditions, we used the approach of

Pfaffl (2001) by calculating the relative expression ratio (R) using the formula $R = [E_{target}^{\wedge}(\Delta CP_{target})] \div [E_{reference}^{\wedge}(\Delta CP_{reference})]$, where $\Delta CP = Ct_{control} - Ct_{sample}$. The $Ct_{control}$ was the Ct value at 2 μM dietary zinc, and the Ct_{sample} was the Ct value at 2 μM–2 mM dietary zinc. The relative expression ratio was determined independently for two reference genes, and the average of these values is represented as a fold change (Figure 5) according to Vandesompele *et al.* (2002).

Analysis of CDF-2::GFP: To determine the expression pattern of CDF-2, we generated the plasmid pDG222 as follows: Beginning with pBluescript SK+ (Stratagene, Santa Clara, CA), we inserted the ~3.4-kb genomic region containing *cdf-2* from 1371 bases upstream to 2006 bp downstream of the ATG (eliminating the stop codon) in frame to the coding region for green fluorescent protein (GFP) and the *unc-54* 3′-UTR, both amplified from pPD95.77, a gift from A. Fire (Stanford University, Palo Alto, CA). Transgenic animals were generated by co-injecting pDG222 and the dominant transformation marker pRF4 (Mello *et al.* 1991) into wild-type animals, selecting F_1 Rol progeny, and selecting three independently derived strains that transmitted the Rol phenotype. For each of these strains, the Rol phenotype was transmitted to only a subset of self-progeny, indicating that these three transgenes are extrachromosomal, and we designated these arrays *amEx1032*, *amEx1033*, and *amEx1201*. To generate plasmid pDP15 for biolistic transformation, we modified the plasmid pMM016, a gift from J. Austin (Praitis *et al.* 2001), that contains *unc-119(+)* by digesting it with *Acc*651 and *Hin*cII and inserting an ~4.8-kb *Eag*I/*Acc*651 fragment of pDG222 containing the *cdf-2* promoter and coding region, *gfp*, and the *unc-54* 3′-UTR. Biolistic transformation was used to introduce pDP15 into *unc-119(ed3)* mutant animals (Praitis *et al.* 2001). Three independently derived transgenic animals that were non-Unc and segregated only non-Unc progeny were isolated. Since the *unc-119* transgenes were transmitted to all the progeny of these three strains, the transgenes are likely to be integrated in the genome and were designated *amIs2*, *amIs4*, and *amIs5*.

To analyze the distribution of GFP using an anti-GFP antibody, we followed the protocol described by Duerr (2006). Briefly, we cultured animals on NGM with live *E. coli*, collected mixed-stage animals, washed in M9 buffer, fixed in methanol and acetone, rehydrated through 90, 60, 30, and 10% acetone, blocked in 5% bovine serum albumin in phosphate-buffered saline with 0.5% Triton X-100, stained with 1:100 dilution of Molecular Probes rabbit anti-GFP primary antibody (A11122, Invitrogen) and 1:200 dilution of Molecular Probes Alexa Fluor 488 goat anti-rabbit secondary antibody (A11008, Invitrogen), and visualized the fluorescence using a Zeiss Axio Imager Z1 (Oberkochen, Germany). GFP localization in live animals was analyzed using the same culture conditions by directly visualizing GFP fluorescence.

Analysis of *cdf-2(tm788)*: *cdf-2(tm788)* was a gift of the Mitani laboratory (National Bioresource Project, Tokyo Women's Medical University, Tokyo). *cdf-2(tm788)* was backcrossed to wild type four times. To eliminate potential mutations linked in *cis* to *cdf-2(tm788)* on chromosome X, we created a triple mutant of *cdf-1(n2527) cdf-2(tm788) sur-7(ku119)*, crossed the strain to wild type, and selected *cdf-1(+) cdf-2(tm788) sur-7(+)* animals. The *cdf-2(tm788)* molecular lesion was analyzed by determining the DNA sequence of the PCR-amplified *cdf-2* locus.

RESULTS

The use of completely defined, axenic medium to manipulate dietary zinc: The most commonly used culture medium for *C. elegans* is NGM that is dispensed in a Petri dish and seeded with a bacterial lawn of *E. coli* (Brenner 1974). NGM provides nutrients for *E. coli* growth, and the worms obtain nutrients by eating the *E. coli*. In these growth conditions, worms develop from egg to adult in ~3.5 days at 20° and generate ~300 self-progeny in the first 5 days of adulthood (Riddle *et al.* 1997). In our initial attempts to manipulate dietary zinc, we supplemented NGM with zinc sulfate and seeded this medium with *E. coli* (Bruinsma *et al.* 2002). *cdf-1(n2527)* mutant animals displayed dose-dependent impairment of growth, indicating these medium conditions resulted in increased dietary zinc. However, zinc was not highly soluble in NGM, limiting the utility of this approach. To address the limitation of zinc solubility, we developed a culture medium that allowed effective supplementation with zinc sulfate, which we named noble agar minimal media (NAMM) (Bruinsma *et al.* 2008). Culture conditions involving NGM and NAMM have two significant limitations. First, the worms consume *E. coli*, which is a food source with a level of zinc that is undefined and difficult to manipulate. Second, while these cultures can be supplemented with zinc, these conditions do not permit depletion of dietary zinc. To overcome these limitations, we used CeMM, a completely defined, axenic, liquid medium (Szewczyk *et al.* 2003). CeMM is formulated from purified vitamins, growth factors, amino acids, nucleic acids, heme, β-sitosterol, sugar, salts, and trace metals. CeMM provides adequate nutrition for indefinite propagation of *C. elegans* cultures (Szewczyk *et al.* 2003). Compared to worms cultured on NGM with live *E. coli*, worms cultured in CeMM display phenotypes suggestive of mild nutrient deprivation, such as delayed development, an extended life span, diminished self-fertile brood sizes, and a thin adult body morphology. However, the proportion of the life cycle spent in each larval stage is similar in both media conditions (Szewczyk *et al.* 2003, 2006).

Standard CeMM contains 75 μM zinc chloride (Szewczyk *et al.* 2003). To use this medium to manipulate dietary zinc, we prepared CeMM with no added zinc chloride (See materials and methods). To determine the level of zinc contamination in the medium components, we used ICP-MS to measure zinc. Medium that was formulated with no added zinc contained ~30 ± 18 parts per billion by weight zinc (mean of seven independent medium preparations). This corresponds to ~0.25 μM zinc, indicating that there is minimal zinc contamination in the medium components.

Maturation and population growth of wild-type worms required a minimal level of dietary zinc and were inhibited by high dietary zinc: To determine how dietary zinc affects the development and maturation of worms, we cultured worms on NGM dishes with live *E. coli* and transferred eggs to CeMM with 18–19 different concentrations of zinc, ranging from no added zinc to 2 mM zinc (Figure 1A). Development was monitored after 80% of wild-type animals matured to adulthood

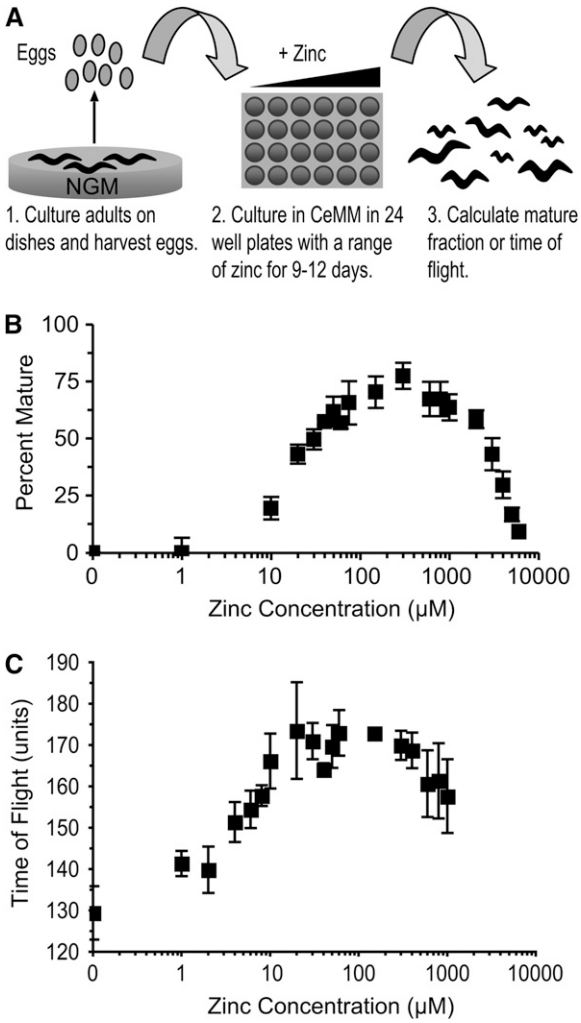

Figure 1.—The maturation of wild-type worms is affected by dietary zinc. (A) To monitor maturation, we cultured adults on NGM with live *E. coli*, transferred eggs or L1 larvae to CeMM (18–19 different zinc concentrations) in 24-well plates, cultured for 9–12 days, and evaluated maturation using a dissecting microscope (B) or a COPAS Biosort (C). (B) Wild-type worms were cultured in CeMM with added zinc, displayed on a logarithmic scale. To calculate the percentage of eggs that matured to an adult, we counted immature and mature animals and calculated the percentage of mature animals. (C) Maturation was monitored using the COPAS Biosort to measure time of flight (TOF). TOF is a measure of the time that the animal blocks light transmission and is shown in arbitrary units. The TOF value of animals at the beginning of the experiment was ~80 units. Values are the average (± standard deviation, SD) of four biological replicates.

with optimal concentrations of zinc, which required 9–12 days in culture (Figure 1B). Initially, maturation was monitored using a dissecting microscope, and animals were scored as larvae or adults. To automate the analysis, we employed a COPAS Biosort instrument that evaluates each animal with a laser microbeam and measures time of flight (TOF) and extinction (EXT). Time of flight measures the time necessary for the animal to flow past the laser, which is an indication of the length of the animal. Extinction measures the percentage of light transmission that is blocked during the time of flight, which is an indication of the width and optical density of an animal. Time of flight and extinction are highly correlated, and both measurements indicate the size and maturity of an animal, with high values indicating a larger, more mature animal (Pulak 2006). Figure 1, B and C show that maturation is strongly affected by dietary zinc. At concentrations of 0 and 1 μM zinc, worms displayed minimal maturation. At concentrations from 2 μM to 15 μM zinc, worms displayed measurable but impaired maturation. Worms displayed maximal maturation in 30 μM to 200 μM zinc and did nearly as well up to ~500 μM zinc. At zinc concentrations >500 μM, worms displayed concentration-dependent impairment of growth.

The maturation assay evaluates development and growth from the egg or L1 larva to the adult stage. To examine the complete life cycle, including reproductive performance, we analyzed the growth rate of a population (Figure 2A). Worms were cultured in CeMM containing 30–75 μM zinc for multiple generations, since these concentrations are in the range for maximal growth. Worms were transferred to CeMM containing 16 different zinc concentrations ranging from no added zinc to 2.5 mM zinc. To determine the maximum growth rate for the population, we counted the number of worms in the population at several times after transfer to the new medium. Population growth was approximately linear between 7 and 17 days in culture (Figure 2B). Overall the results were similar to the maturation assay. With no added zinc, there was no significant population growth (Figure 2, C and D). With 1 μM to 2 μM added zinc, there was measurable but severely impaired population growth. From 2 μM to 30 μM zinc, there was a dose-dependent increase in population growth. To quantify these data, we determined the effective concentration (EC_{50}) of zinc that resulted in a population growth rate that was half the maximal population growth rate. The EC_{50} for wild-type animals was 6.8 ± 1.1 μM zinc (Table 1). From 30 μM to 1 mM zinc, there was relatively optimal population growth (Figure 2, C and D). Concentrations >1 mM caused a reduction of population growth rates. We determined the inhibitory concentration (IC_{50}) of zinc, and the IC_{50} for wild-type animals was 1.3 ± 0.3 mM zinc (Table 1). These results indicate that worms require dietary zinc for efficient maturation and reproduction, thrive in a wide range of dietary zinc concentrations from 30 μM to 1 mM, and are susceptible to zinc toxicity at concentrations above 1 mM.

Zinc content of wild-type worms is correlated with dietary zinc: To complement the analysis of how dietary zinc affects maturation and population growth, we developed two methods to measure the zinc content of animals. The first method utilized radioactive ^{65}Zn. Animals were cultured with a range of dietary zinc and a trace amount of ^{65}Zn, the amount of internalized ^{65}Zn

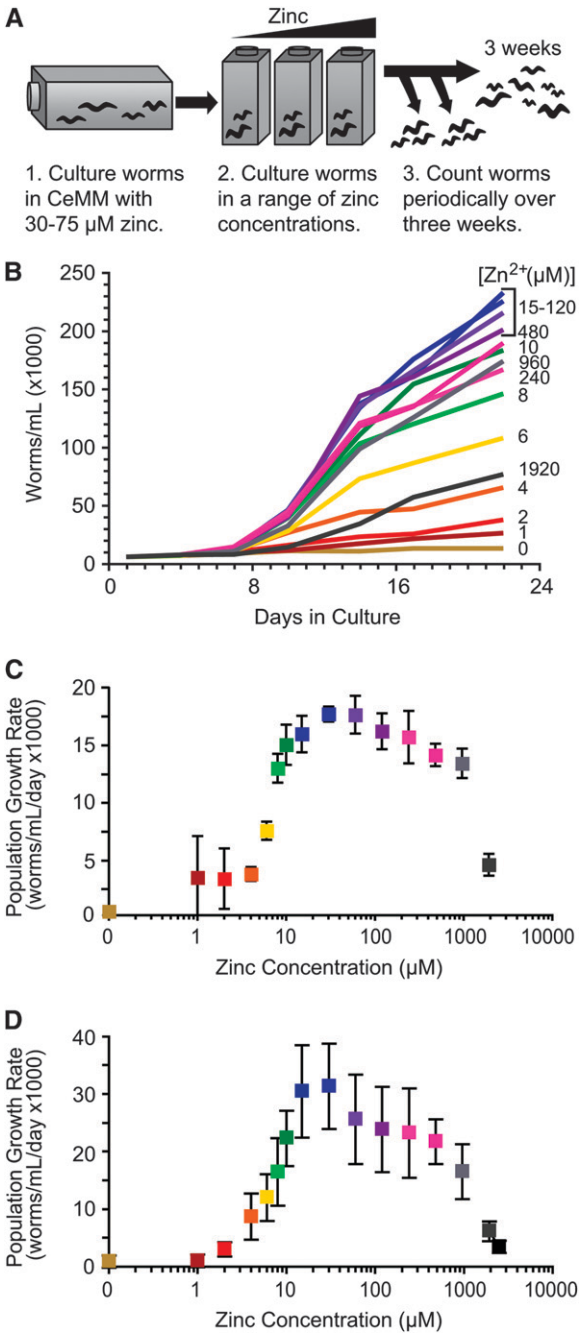

FIGURE 2.—The population growth rate of wild-type worms is affected by dietary zinc. (A) To monitor the growth rate of the population, we cultured worms in CeMM with 30–75 μM zinc for multiple generations, transferred worms to flasks of CeMM (15–16 different zinc concentrations), and counted the number of worms per milliliter of culture medium at multiple times. Counting was performed using a dissecting microscope (B and C) or a COPAS Biosort (D). (B) Wild-type worms were cultured in CeMM with different concentrations of added zinc shown in micromolars and indicated by colored lines. The numbers of worms per milliliter were determined at culture days 1, 4, 7, 10, 14, 17, and 22. The increase in population was maximal and approximately linear between days 7 and 17. (C) The slopes of the lines defined by the linear range shown in B were used to calculate population growth rates in worms/ml/day. The concentration of added zinc is displayed on a logarithmic scale. The colors of the data points correspond to the colors of the lines shown in B. Values are the average (±SD) of three independent experiments, one of which is shown in B. (D) Population growth rate was monitored using the COPAS Biosort to measure the number of animals at four time points between days 9 and 17. Values are the average (±SD) of three independent experiments. The growth rates calculated from the COPAS Biosort data are somewhat higher than the growth rates calculated from the dissecting microscope data, probably because human observers are more stringent than the instrument in scoring an object as a worm. Nonetheless, the effect of zinc on population growth rate was similar when measured using a dissecting microscope or the COPAS Biosort.

was determined using a gamma counter, and the sample size was determined by measuring the protein concentration. The second method utilized ICP-MS, a technique that can measure the concentration of several different elements in a single sample, including zinc. Worms were cultured with a range of dietary zinc, the metal content was determined by ICP-MS, and the dry weight was determined to establish the sample size. Both methods demonstrated that the zinc content of wild-type *C. elegans* was strongly influenced by the level of dietary zinc (Figure 3A and supporting information, Table S1). Worms cultured in 6 μM zinc had a zinc content of ~40 ppm, whereas worms cultured in 2 mM zinc had a zinc content of ~1000 ppm, a 27-fold difference. By contrast, the content of three other physiologic metals, iron, copper, and manganese, was not strongly affected by dietary zinc (Figure 3B). The iron content displayed minimal change, and copper and manganese contents declined <2-fold. Figure 3C shows that when the zinc content of wild-type animals increased above ~400 ppm there was a corresponding decrease in population growth rate that was caused by high concentrations of dietary zinc.

While an increase in dietary zinc always resulted in an increase in total zinc content, the quantitative relationship between the change in zinc content and the change in dietary zinc (the slope) displayed an interesting pattern. Figure 3D shows that at the lowest concentrations of dietary zinc (6–10 μM), the zinc content displayed the greatest change in response to increased dietary zinc (3.4 ppm/μM). As the dietary zinc concentration was increased to an optimal level (75–350 μM), the rate of change of zinc content progressively decreased to 0.6 ppm/μM. As the dietary zinc concentration was increased to toxic levels (1–2 mM), the rate of change of zinc content was relatively stable (0.4–0.5 ppm/μM). These results indicate that worms cultured in low concentrations of zinc undergo robust changes in zinc content when additional dietary zinc is provided, whereas worms cultured in high concentrations of zinc are resistant to changes in zinc content when challenged with additional dietary zinc. However, wild-type worms continued to accumulate zinc even at toxic concentrations of dietary zinc >1 mM.

TABLE 1

Quantitative analysis of zinc requirements and toxicities

Strain[a]	EC_{50}	IC_{50}
WT	6.8 ± 1.1	1300 ± 290
cdf-1	5.1 ± 0.65	550 ± 350
cdf-2	3.8 ± 0.99	1900 ± 160
sur-7	5.1 ± 1.3	640 ± 170*
cdf-1 cdf-2	5.7 ± 0.05	580 ± 170*
cdf-2 sur-7	7.0 ± 0.50	480 ± 47*
cdf-1 sur-7	7.2 ± 1.3	600 ± 290
cdf-1 cdf-2 sur-7	7.9 ± 0.30	220 ± 13*

Values are dietary zinc concentrations in micromolars (average ± SD of two to three independent experiments). Values significantly different from WT ($P < 0.05$, Welch's *t*-test) are indicated with an asterisk.

[a] Mutant alleles were *cdf-1(n2527)*, *cdf-2(tm788)*, and *sur-7(ku119)*.

C. *elegans* *cdf-2* encodes a member of the cation diffusion facilitator family: Vertebrates contain CDF proteins localized to the plasma membrane, ZnT-1, and to vesicular membranes, ZnT-2, ZnT-3, ZnT-4, and ZnT-8 (Palmiter and Findley 1995; Gaither and Eide 2001; Kambe *et al.* 2004). We demonstrated previously that *C. elegans* CDF-1 is most similar to the vertebrate ZnT-1 subfamily by sequence criteria and by the experimental observation that ZnT-1 can functionally substitute for CDF-1 (Bruinsma *et al.* 2002). To investigate a *C. elegans* cation diffusion facilitator protein that is closely related to the ZnT-2, ZnT-3, ZnT-4, and ZnT-8 subfamily, we initiated an analysis of the predicted gene T18D3.3. The computer algorithm Gene Finder predicted that the T18D3.3 gene contains eight exons and encodes a protein of 360 amino acids, and we experimentally validated the predicted gene structure (Figure 4A and materials and methods). The predicted T18D3.3 protein contains hallmarks of the CDF family including six transmembrane-spanning segments and two histidine motifs, $(HX)_3$, in the loop between the fourth and fifth transmembrane segments (Figure 4B), and we thus named it CDF-2. Compared to vertebrate proteins, CDF-2 is most similar to ZnT-2, which is localized to intracellular vesicles and is involved in zinc secretion into breast milk (Palmiter *et al.* 1996a; Chowanadisai

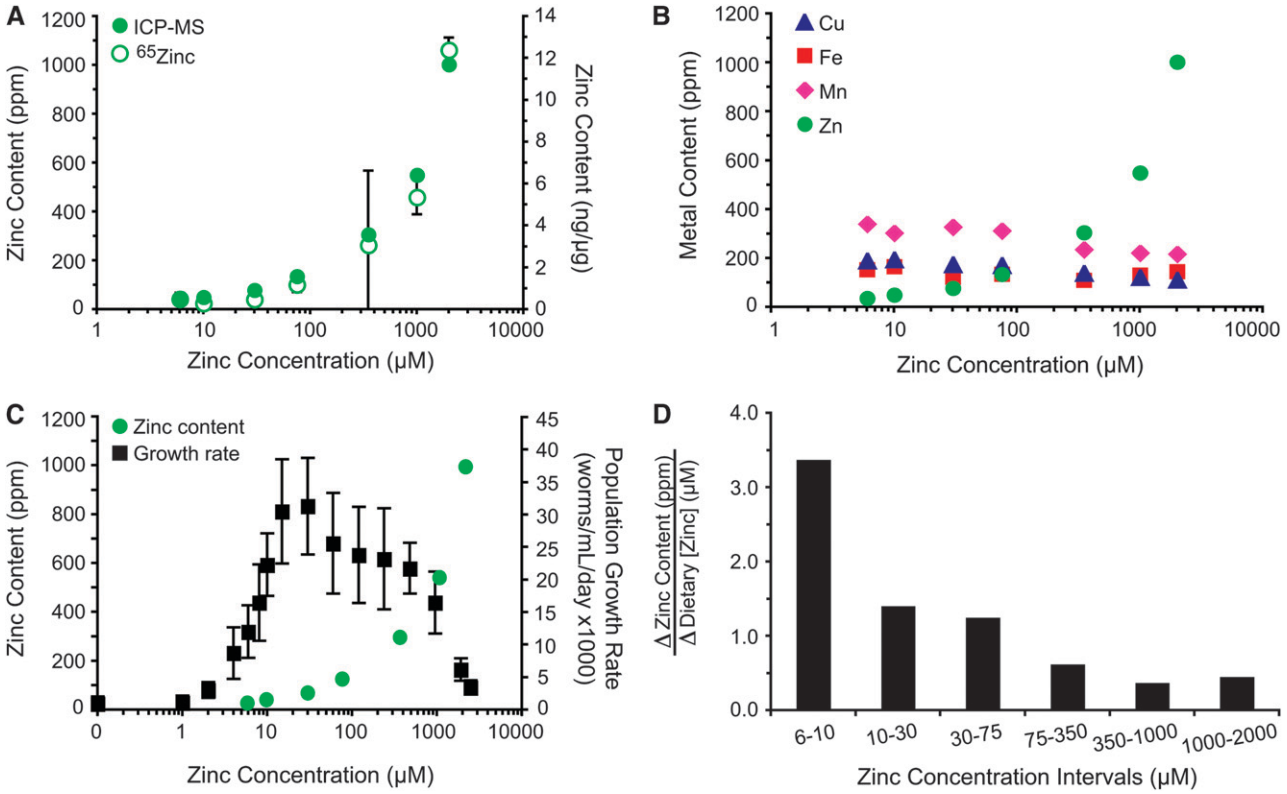

Figure 3.—Zinc content of mixed-stage wild-type animals. Worms were cultured in CeMM with a range of added zinc, shown on a logarithmic scale. (A) The zinc content was determined by ICP-MS (ppm, closed green circles), or radiolabeled ^{65}Zn (average ng zinc/µg protein ± SD, $n = 2$, open green circles) in independent experiments. (B) ICP-MS was used to measure the content of copper (Cu, blue triangles), iron (Fe, red squares), manganese (Mn, pink diamonds), and zinc (Zn, green circles) of each sample. The dietary concentrations of copper, iron, and manganese in CeMM were 37.5 µM, 150 µM, and 112.5 µM, respectively, in all the samples. (C) Zinc content was determined by ICP-MS (green circles), and population growth rate was determined by COPAS Biosort (black squares) in independent experiments. (D) Bars indicate the change in zinc content (ppm) divided by the change in dietary zinc (µM) for the two dietary zinc concentrations shown below. Values are the slope of the line defined by the ICP-MS data in A.

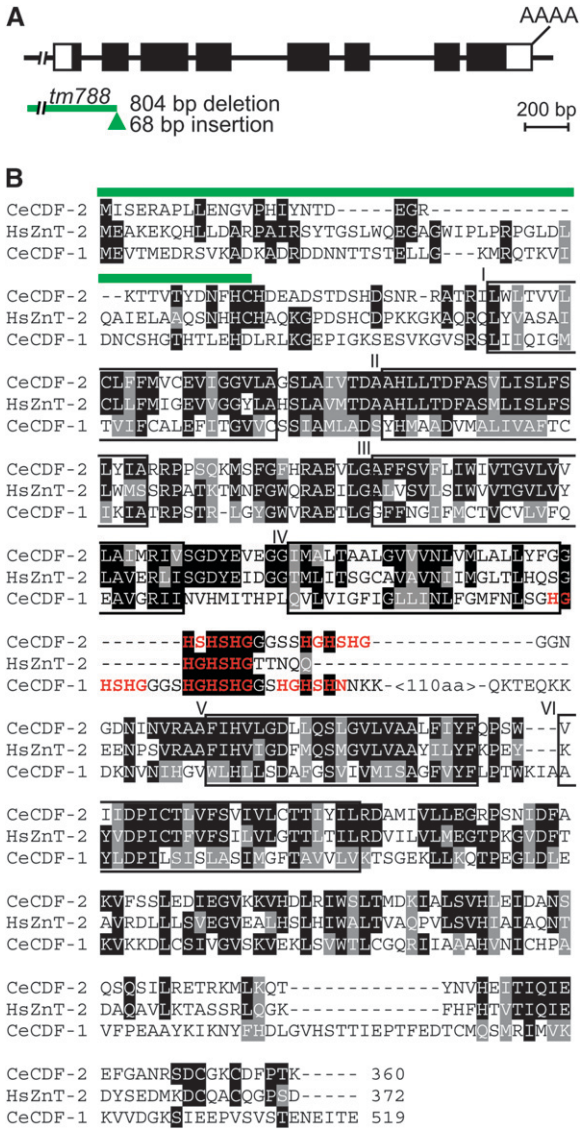

FIGURE 4.—*cdf-2* gene structure and predicted amino acid sequence. (A) The line represents genomic DNA, and boxes represent exons that are untranslated (white) or translated (black). The green line indicates the extent of the *tm788* deletion, and the green triangle denotes the *tm788* insertion. (B) An alignment of the predicted CDF-2 protein with human ZnT-2 and *C. elegans* CDF-1. Identical and similar amino acids are highlighted in black and gray, respectively. Green lines indicate codons deleted in the *tm788* allele. Putative zinc binding motifs, $(HX)_n$, are red. Predicted transmembrane segments are boxed and labeled I–VI.

et al. 2006). While these sequence similarities indicate that CDF-2 functions as a zinc transporter, the biochemical activity of CDF-2 has not yet been demonstrated experimentally.

***cdf-2* transcript levels were regulated by dietary zinc:** To investigate how dietary zinc regulates the expression of *cdf-2*, we used quantitative, real-time PCR to monitor the abundance of *cdf-2* mRNA. Wild-type worms were cultured in CeMM with added zinc chloride for 6 days to achieve stable gene expression. Adult animals were collected, and the abundance of *cdf-2* transcripts was determined. For comparison, the abundances of *cdf-1* and *sur-7* transcripts were also determined. The abundances of transcripts from these genes were normalized to the abundance of two genes that displayed stable expression over a range of zinc concentrations, *ama-1* and *rps-23* (data not shown).

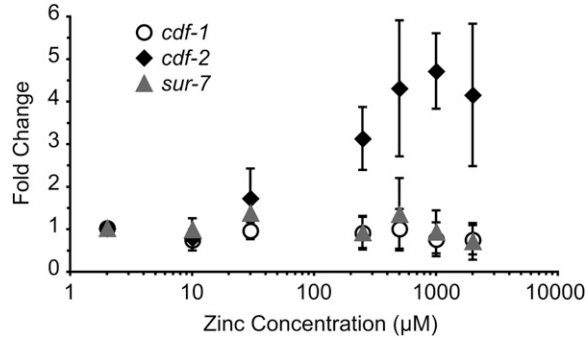

FIGURE 5.—*cdf-2* transcript abundance was regulated by dietary zinc. Wild-type animals were cultured in CeMM with added zinc, shown on a logarithmic scale. The abundance of transcripts from *cdf-1* (open circles), *cdf-2* (solid diamonds), and *sur-7* (shaded triangles) was measured by performing quantitative, real-time PCR. The axis represents the fold change in transcript abundance, which was calculated by comparing the transcript abundance at 2 μM, 10 μM, 30 μM, 250 μM, 500 μM, 1 mM, and 2 mM dietary zinc to transcript abundance at 2 μM dietary zinc. Values for transcript abundance were corrected for RNA recovery and the efficiency of primer amplification (see MATERIALS AND METHODS). The fold change of each gene at 2 μM zinc was set equal to 1.0, and other values were normalized relative to 2 μM zinc. Values are the average of four independent replicates (±SD). Compared to transcript abundance at 2 μM zinc, *cdf-2* transcripts were significantly higher at zinc concentrations of 250 μM to 2 mM zinc (approximately three- to fourfold, $P < 0.05$, Welch's *t*-test), whereas *cdf-1* and *sur-7* transcripts were significantly decreased at 2 mM zinc (approximately twofold, $P < 0.05$, Welch's *t*-test).

At the low concentration of 2 μM zinc, *cdf-1* transcripts were most abundant, *cdf-2* transcripts were intermediate in abundance, and *sur-7* transcripts were least abundant (data not shown). As the concentration of dietary zinc was increased, the abundance of *cdf-2* transcripts increased progressively, displaying about twofold induction at 30 μM zinc and three- to fourfold induction at 250 μM to 2 mM zinc (Figure 5). By contrast, the abundances of *cdf-1* and *sur-7* transcripts were not increased. At the high concentration of 2 mM zinc, *cdf-2* transcripts were more abundant than *cdf-1* or *sur-7* transcripts. These findings suggest that *cdf-2* has an important function in the response to increased dietary zinc.

CDF-2 localized to vesicles in intestinal cells: To determine the cells that express CDF-2 and the subcellular localization of the protein, we expressed a CDF-2::GFP fusion protein under the control of the predicted *cdf-2* promoter in transgenic worms. In an

attempt to include all the relevant promoter elements that might mediate cell-type specific expression, we designed the reporter construct to include 1371 bp upstream of the predicted initiation codon, the entire open reading frame, and all of the introns. To include all of the relevant protein domains that might mediate subcellular localization, we included the entire CDF-2 protein sequence. The plasmids were introduced into wild-type animals by microinjection to yield extrachromosomal arrays (Mello *et al.* 1991) and into *unc-119(ed3)* mutant animals by biolistic bombardment to yield integrated arrays (Praitis *et al.* 2001). To determine the reproducibility of the observed expression patterns, we identified six independently derived transgenic lines. The expression pattern of CDF-2::GFP was similar in all six independently derived transgenic lines, indicating that this pattern is not influenced by the genomic integration sites or by rearrangements that may have occurred during the formation of extrachromosomal arrays. In wild-type animals, the intestinal cells contain granules that display autofluorescence. Autofluorescence is first detected in embryos and becomes progressively more intense as animals mature. Live CDF-2::GFP transgenic worms appeared to display enhanced fluorescence in embryos compared to wild-type worms. As animals matured and the intestinal granules displayed more intense autofluorescence, we could no longer observe enhanced fluorescence in live CDF-2::GFP transgenic worms. Because autofluorescence of intestinal granules made it difficult to observe CDF-2::GFP, we fixed embryos and animals, a process that eliminates autofluorescence, and visualized CDF-2::GFP using an anti-GFP antibody. CDF-2::GFP was expressed in embryos (Figure 6, E–L), larvae (Figure 6, M–P), and adults (Figure 6, Q–T). The CDF-2::GFP protein was expressed in intestinal cells in a punctate pattern that appears to be the membrane of small vesicles (Figure 6U). To investigate the relationship between the punctate pattern of CDF-2::GFP and the punctate pattern of autofluorescent intestinal granules, we analyzed fluorescence in live adult worms (Figure 6, A–D). These results indicate that CDF-2::GFP is only expressed in puncta that are autofluorescent. These data are consistent with the possibilities that all or only some of the autofluorescent puncta contain CDF-2::GFP, and suggest that CDF-2::GFP is not expressed outside of autofluorescent puncta. A CDF-1::GFP fusion protein is also expressed in intestinal cells, but it is localized to the plasma membrane (Bruinsma *et al.* 2002), and it is not localized to the vesicles that contain CDF-2. Therefore, the subcellular localization of CDF-2::GFP is unlikely to be mediated by the GFP fusion partner and appears to be specific for CDF-2. While the CDF-2::GFP fusion protein was designed to indicate the expression pattern of endogenous CDF-2, the function of the CDF-2::GFP fusion protein has not been analyzed, and it is possible that endogenous CDF-2 is expressed in a broader or more restricted pattern than the CDF-2::GFP reporter. These results indicate that CDF-2 is localized to vesicular membrane compartments similar to the related vertebrate proteins ZnT-2, ZnT-3, Znt-4, and ZnT-8 (Gaither and Eide 2001; Kambe *et al.* 2004).

A *cdf-2* loss-of-function mutation resulted in delayed population growth and decreased zinc content: To investigate the function of *cdf-2*, we obtained the *tm788* deletion allele from the Mitani laboratory (National Bioresource Project, Tokyo). We determined the sequence of the *cdf-2* locus and confirmed that *tm788* is an 804-bp deletion that removes 594 bp upstream of the ATG, exon 1, intron 1, and 69 bp of exon 2 (Figure 4A). In addition, there is a 68-bp insertion at the site of the deletion. The deleted DNA encodes the first 34 predicted amino acids of the CDF-2 protein. The *tm788* deletion is predicted to affect the *cdf-2* transcript in two important ways. First, *tm788* is predicted to reduce the abundance of *cdf-2* transcripts by removing the 5′ upstream region that might contain promoter elements and the transcription initiation site. Second, any *cdf-2* transcripts that are produced must have an abnormal structure, since exon 1 and part of exon 2 are absent. Such abnormal transcripts would definitely lack the codons for the first 34 predicted amino acids and might lack additional codons. The first methionine codon in the *cdf-2* open reading frame that remains in the *tm788* mutant is codon 65, and a protein that initiated at codon 65 would lack half of the highly conserved first transmembrane domain.

To determine how the *cdf-2(tm788)* mutation affects the abundance of the *cdf-2* transcript, we used the sensitive method of reverse transcription–PCR. The abundance of the *cdf-2* transcript was dramatically reduced by ~1000-fold in the *cdf-2(tm788)* mutant compared to wild type, and the residual *cdf-2* transcript was not induced by dietary zinc (Figure S1). These findings indicate that the *cdf-2(tm788)* deletion eliminates sequences that are critical for transcript initiation and/or sequences in the transcribed region that are critical for transcript stability. These results suggest that the *cdf-2(tm788)* mutation causes a strong loss of function.

To analyze the phenotype of the *cdf-2(tm788)* mutant, we first backcrossed the strain to wild-type animals to remove extraneous mutations. *cdf-2(tm788)* mutant animals appeared to have normal morphology and body movement. *cdf-2(tm788)* did not cause significant lethality, and *cdf-2(tm788)* hermaphrodites and males were fertile (data not shown). The *cdf-2(tm788)* mutation did not suppress the multivulval phenotype caused by constitutively activated *let-60(n1046)* Ras (data not shown), by contrast to loss-of-function mutations of *cdf-1* and *sur-7* (Bruinsma *et al.* 2002; Yoder *et al.* 2004). To carefully monitor the ability of *cdf-2(tm788)* mutant animals to grow and develop in a wide range of dietary

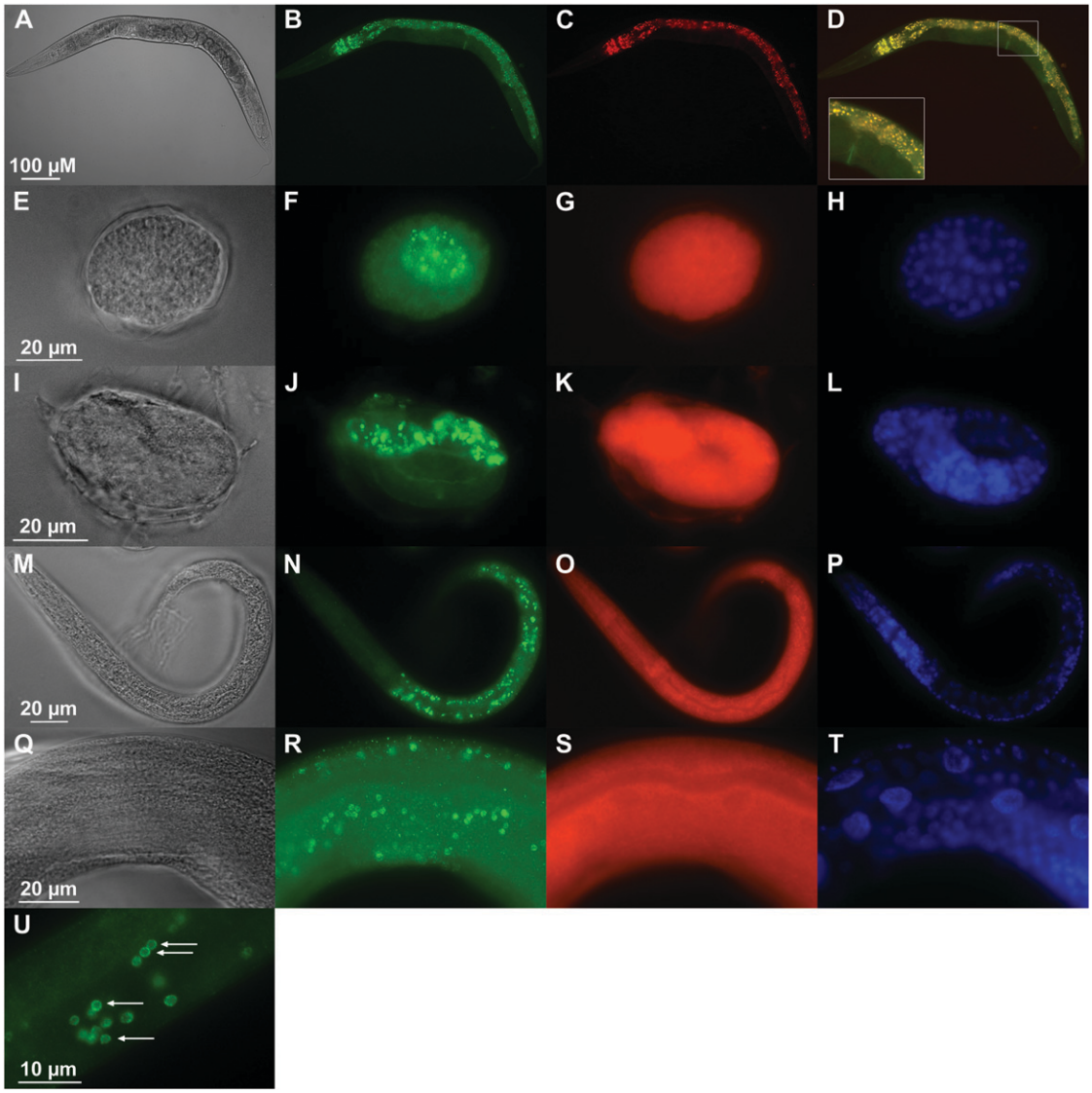

FIGURE 6.—CDF-2 was expressed in intestinal cells and localized to membrane-bound vesicles. Transgenic animals expressing CDF-2::GFP were cultured on NGM with live *E. coli*. Live adults were immobilized and mounted (A–D). The inset in D is a 2.4× magnification of the boxed region. Mixed-stage worms were fixed and stained with an anti-GFP antibody (E–U). Differential interference contrast images display organism morphology (A, E, I, M, and Q), green displays CDF-2::GFP and autofluorescence (B) or only CDF-2::GFP (F, J, N, R, and U), red displays autofluorescence (C, G, K, O, and S), yellow displays overlap between CDF-2::GFP and autofluorescence (D), and blue displays nuclear morphology using DAPI (H, L, P, and T). Red in C shows a punctate pattern of autofluorescence in intestinal cells, whereas red in G, K, O, and S shows that there is no specific localization of autofluorescence following fixation, and exposure times for red in these panels were at least fivefold longer than for green. CDF-2::GFP was first detected during embryogenesis at the E^{16}–E^{20} stage (F), and expression persisted throughout embryogenesis (J). CDF-2::GFP was expressed in a punctate pattern in intestinal cells during all larval stages (N) and in adults (R). Puncta appear to be membrane-bound vesicles (arrows in U).

zinc conditions, we used CeMM to conduct maturity and population growth assays. Figure 7A shows that maturation from L1 to adult was similar for *cdf-2(tm788)* mutant and wild-type animals in a wide range of dietary zinc. By contrast, *cdf-2(tm788)* mutant animals displayed reduced population growth compared to wild-type animals in 30–480 μM dietary zinc (Figure 7B). In extremely low and high dietary zinc conditions, *cdf-2(tm788)* mutant and wild-type animals displayed similar population growth, and the EC_{50} and IC_{50} values for *cdf-2(tm788)* mutant animals were 3.8 ± 1.0 μM zinc and 1900 ± 160 μM zinc, respectively (Table 1). These findings indicate that *cdf-2* is necessary for wild-type levels of population growth when dietary zinc is in the optimal range.

To determine how *cdf-2* influences zinc content, we analyzed *cdf-2(tm788)* mutant animals using ICP-MS. Figure 7C shows that *cdf-2(tm788)* mutant animals displayed reduced zinc content at dietary zinc concentrations of ≥30 μM compared to wild-type animals (Table S1); at a dietary zinc concentration of 75 μM,

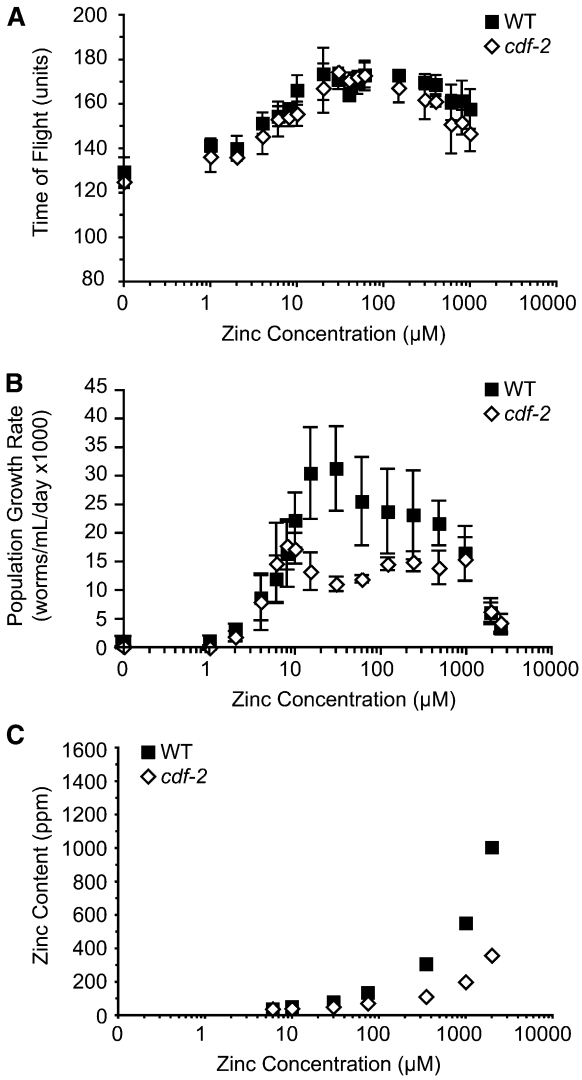

FIGURE 7.—*cdf-2* mutant phenotypes. Wild-type and mutant animals were cultured in CeMM with a range of added zinc, shown on a logarithmic scale. (A) Maturation of wild type (WT, solid squares) and *cdf-2(tm788)* (open diamonds) was monitored using the COPAS Biosort. Values are the average (±SD) of four biological replicates and are representative of two independent experiments. (B) Population growth rate was monitored using the COPAS Biosort, and values are the average (±SD) of two to three independent experiments. (C) Zinc content was measured using ICP-MS.

the zinc content of the *cdf-2* mutant was reduced twofold, and at dietary zinc concentrations of 350 μM, 1 mM, and 2 mM the zinc content of the *cdf-2* mutant was reduced threefold. In conjunction with the localization data, these results suggest that CDF-2 functions to store zinc in vesicles of intestinal cells.

Loss-of-function mutations in *cdf-1* and *sur-7* affect sensitivity to dietary zinc and zinc content: *cdf-1* and *sur-7* are critical for Ras-mediated signal transduction and resistance to high levels of dietary zinc when animals are cultured with live *E. coli* (BRUINSMA *et al.* 2002; YODER *et al.* 2004). The role of these genes in conditions of low dietary zinc has not been determined. We used CeMM to analyze the functions of *cdf-1* and *sur-7* in a full range of dietary zinc. The strong loss-of-function *cdf-1(n2527)* mutation is a nonsense change that is predicted to truncate the protein at amino acid 156 of 519, resulting in the absence of three highly conserved transmembrane domains (BRUINSMA *et al.* 2002). The partial loss-of-function *sur-7(ku119)* mutation affects a predicted splice site and reduces but does not eliminate *sur-7* transcripts (YODER *et al.* 2004). We cultured *cdf-1* and *sur-7* mutant animals in a wide range of dietary zinc and measured the ability of L1 larvae to mature to adulthood. Both *cdf-1* and *sur-7* mutant animals displayed reduced maturation at low and high concentrations of zinc, whereas they displayed wild-type levels of maturation at intermediate zinc concentrations (Figure 8, A and B). Both *cdf-1* and *sur-7* mutant animals displayed reduced population growth at concentrations of dietary zinc from 10 μM to 2.5 mM (Figure 8, C and D). The EC_{50} for population growth rate was similar for these mutant animals and wild type, whereas the IC_{50} was reduced for both *cdf-1* and *sur-7* mutant animals (Table 1). These results indicate that *cdf-1* and *sur-7* are necessary for optimal maturation in low dietary zinc, a result that has not been previously reported. These genes are necessary for optimal population growth in a wide range of dietary zinc and are essential for survival at high dietary zinc, consistent with previous reports (BRUINSMA *et al.* 2002, 2008; YODER *et al.* 2004).

To determine the role of *cdf-1* and *sur-7* in regulating zinc content, we analyzed loss-of-function mutant animals using ICP-MS. *cdf-1* mutant animals displayed increased zinc content at dietary zinc concentrations of ≥30 μM (Figure 8E and Table S1). *sur-7* mutant animals displayed a zinc content similar to wild type (Figure 8F and Table S1). The finding that *sur-7* mutant animals displayed dramatic growth defects and relatively normal zinc content suggests that the distribution of zinc is abnormal in mutant animals. This analysis shows that *cdf* genes can have strikingly different effects on zinc content; *cdf-2* promotes zinc accumulation, whereas *cdf-1* inhibits zinc accumulation.

Analysis of *cdf-1*, *cdf-2*, and *sur-7* double and triple mutant animals: To investigate the genetic interactions between these three genes, we generated the three possible double mutant strains and the triple mutant strain and measured maturation, population growth, and zinc content of each strain (Table 1, Table S1, Table S2, Table S3). The *cdf-1 cdf-2* and *cdf-1 cdf-2 sur-7* mutant animals were particularly informative (Figure 9). Loss-of-function mutations in *cdf-1* and *cdf-2* have opposite effects on zinc content. The *cdf-1 cdf-2* double mutant displayed a zinc content that was intermediate between the two single mutant strains (Figure 9E). The *cdf-1 cdf-2* double mutant had slightly impaired maturation rates compared to the *cdf-1* mutant (Figure 9A), but had slightly improved population growth rates compared to

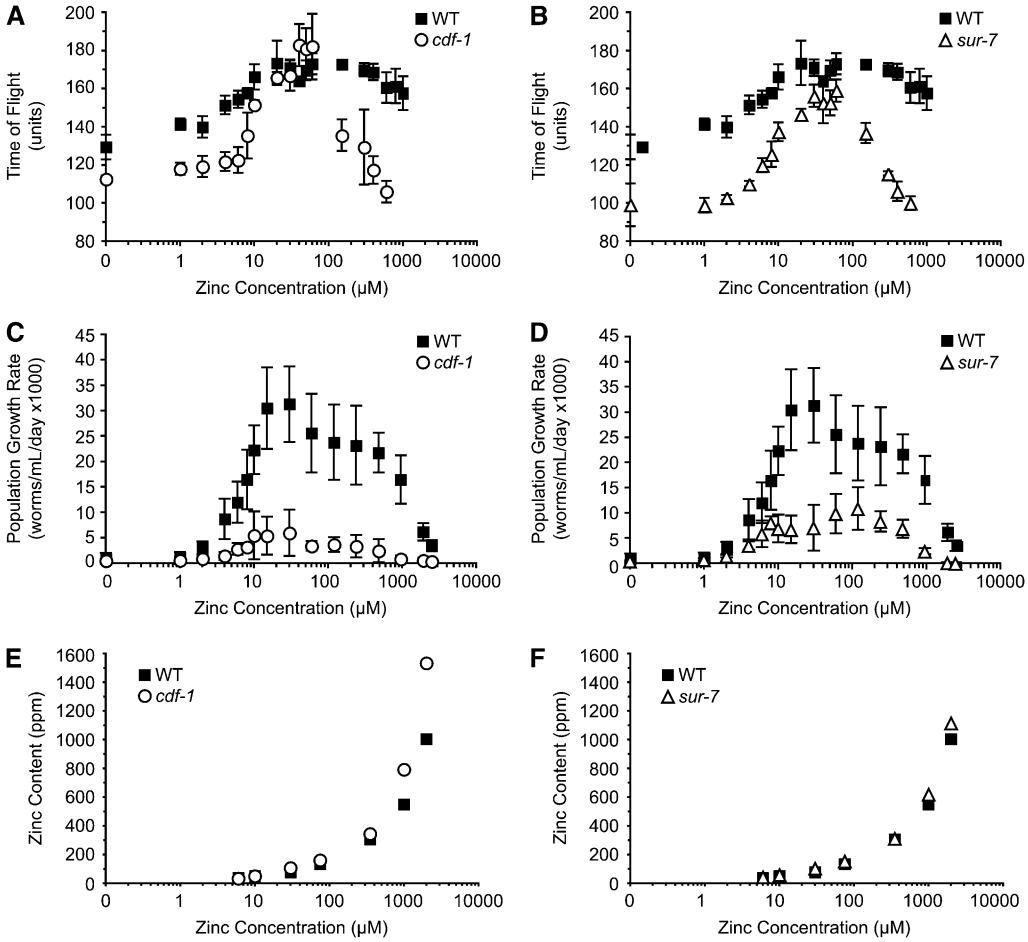

FIGURE 8.—Maturation, population growth rate, and zinc content of *cdf-1* and *sur-7* mutant animals. Wild-type and mutant animals were cultured in CeMM with a range of added zinc, shown on a logarithmic scale. (A and B) Maturation of wild type (WT, solid squares), *cdf-1(n2527)* (open circles), and *sur-7(ku119)* (open triangles) was monitored using the COPAS Biosort. Values are the average (±SD) of four biological replicates and are representative of two independent experiments. (C and D) Population growth rate was monitored using the COPAS Biosort, and values are the average (±SD) of two to three independent experiments. (E and F) Zinc content was measured by ICP-MS.

the *cdf-1* mutant (Figure 9C). These results suggest that *cdf-1* and *cdf-2* have antagonistic functions with respect to zinc content and the more normal zinc content of the *cdf-1 cdf-2* mutant may account for the increase in the population growth rate.

The *cdf-1 cdf-2 sur-7* triple mutant was also intermediate between the *cdf-1* and *cdf-2* single mutant animals with respect to zinc content; furthermore, the *cdf-1 cdf-2 sur-7* mutant had a zinc content that was similar to wild type (Figure 9F). Figure 9G compares the change in zinc content as a function of dietary zinc for single and triple mutant animals. The *cdf-2* single mutant displayed smaller changes in zinc content compared to wild type at all concentrations of dietary zinc. By contrast the *cdf-1* single mutant displayed larger changes compared to wild type in most intervals. Consistent with the interpretation that *cdf-1* and *cdf-2* have antagonistic functions, the values for the triple mutant were usually intermediate between *cdf-1* and *cdf-2* mutant animals. Furthermore, at the highest concentrations of dietary zinc, *cdf-1* and *cdf-1 cdf-2 sur-7* mutant animals displayed a trend toward increasing values in contrast to wild-type animals that displayed decreasing or stable values (Figure 9H). These findings suggest that *cdf* genes are necessary for animals to resist changes in zinc content when challenged with the highest levels of dietary zinc. The *cdf-1 cdf-2 sur-7* mutant had increased population growth rates at optimal dietary zinc concentrations compared to the *cdf-1* mutant, but triple mutant animals were very sensitive to zinc toxicity and had an IC_{50} of 220 μM (Figure 9D and Table 1). The failure of the *cdf-1 cdf-2 sur-7* mutant to control zinc content at high dietary zinc may be responsible for the increased sensitivity to zinc toxicity.

DISCUSSION

Zinc metabolism and homeostasis in wild-type *C. elegans*: *C. elegans* is typically cultured with *E. coli* as a food source, which limits the ability to manipulate dietary constituents such as zinc. Chemically defined media that support long-term culture of the related nematode *C. briggsae* have been developed (BUECHER *et al.* 1966; HIEB and ROTHSTEIN 1968; HIEB *et al.* 1970; LU *et al.* 1978). These culture conditions were adapted for the study of *C. elegans* by LU and GOETSCH (1993), and the growth characteristics of *C. elegans* in fully defined medium were described by SZEWCZYK *et al.* (2003, 2006). To develop culture conditions that allow complete control of dietary zinc, we analyzed worms

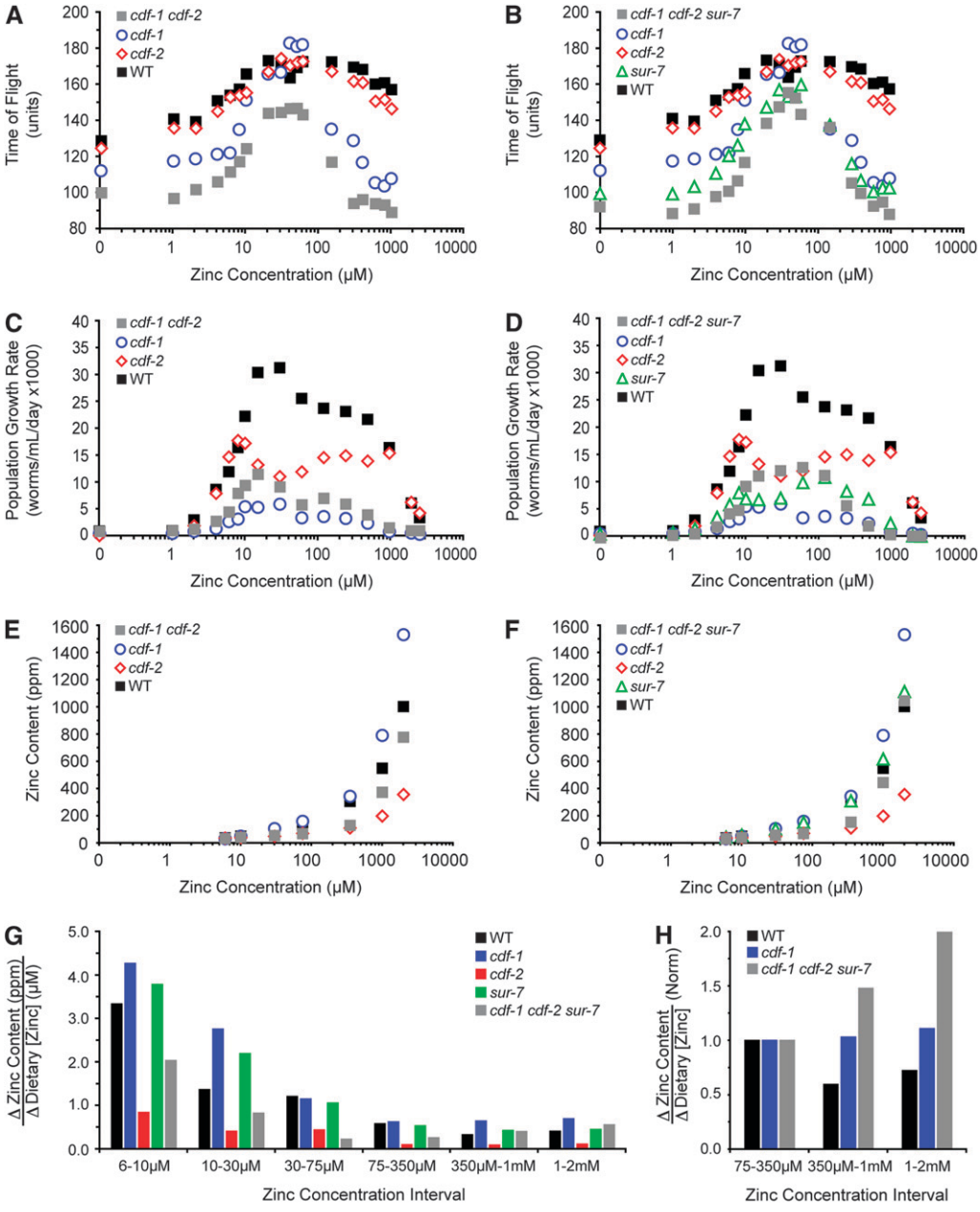

FIGURE 9.—Maturation, population growth rate, and zinc content of double and triple mutant animals. Wild-type and mutant animals were cultured in CeMM with a range of added zinc, shown on a logarithmic scale. (A and B) Maturation of wild type (black squares), *cdf-1(n2527)* (open blue circles), *cdf-2(tm788)* (open red diamonds), *sur-7(ku119)* (open green triangles), *cdf-1(n2527) cdf-2(tm788)* (gray squares), and *cdf-1(n2527) cdf-2(tm788) sur-7(ku119)* (gray squares) was monitored using the COPAS Biosort. Values are the average of four biological replicates. (C and D) Population growth rates were monitored using the COPAS Biosort. Values are the average of two to three independent experiments. Values (±SD) are shown in Table S2 (maturation) and Table S3 (population growth rate). (E–H) Zinc content was measured by ICP-MS. The change in zinc content as a function of change in dietary zinc is displayed in units of ppm/μM (G) or normalized by setting the values for 75–350 μM = 1.0 (H).

using CeMM with no added zinc and a wide range of supplemental zinc. These experiments revealed that *C. elegans* cannot mature or reproduce in CeMM with no added zinc (~0.25 μM zinc), demonstrating that dietary zinc is essential for *C. elegans* survival. When dietary zinc was in the range of 1–10 μM, *C. elegans* displayed impaired but measurable growth, and the EC_{50} for dietary zinc was ~7 μM. When dietary zinc was in the range of 30 μM to 1 mM, *C. elegans* displayed optimal growth. The finding that optimal growth occurs over a 30-fold range in dietary zinc indicates that *C. elegans* have evolved mechanisms to thrive in a relatively broad range of dietary zinc. When dietary zinc was in the range of 1–2.5 mM, *C. elegans* displayed dose-dependent impairment of growth, and the IC_{50} for dietary zinc was ~1.3 mM. The EC_{50} and IC_{50} for dietary zinc differ by 190-fold and define the range of zinc that permits *C. elegans* survival.

The culture conditions described here have important advantages compared to the culture conditions that have been used previously to manipulate dietary zinc (BRUINSMA *et al.* 2002, 2008; YODER *et al.* 2004; DONG *et al.* 2008a). We previously supplemented NGM or NAMM with zinc; these media conditions allowed for supplemental dietary zinc but did not allow for depletion of dietary zinc, since *E. coli* is the food source. The use of CeMM allowed us to quantitatively determine for the first time the minimum, optimum, and maximum dietary zinc levels for *C. elegans*. Similar quantitative measurements of levels have not been systematically

established for other animals, and these studies provide new information about the capacity of multicellular animals to metabolize zinc.

An important method for analyzing zinc metabolism is the measurement of zinc content. The zinc content of *C. elegans* has not been previously reported. We developed two independent methods to measure zinc content. One method employed radioactive ^{65}Zn as a tracer and the second method utilized physical measurements of zinc performed by ICP-MS. Our results indicate that total animal zinc content is proportional to the concentration of dietary zinc. Over the ~30-fold range of dietary zinc that promotes optimal growth (30 μM–1 mM), worms displayed an ~7-fold increase in zinc content. However, the relationship between dietary zinc and zinc content displayed an interesting pattern. At the lowest concentrations of dietary zinc, wild-type worms displayed the most responsiveness to changes in dietary zinc, measured as the change in zinc content per change in dietary zinc. This responsiveness decreased as dietary zinc was increased to the optimal range for population growth and then stabilized as dietary zinc increased to high levels. These findings suggest that at low concentrations of dietary zinc, worms are in a physiological state that promotes uptake of dietary zinc and/or minimizes zinc excretion, so that the animals respond to an increase in dietary zinc with a robust increase in zinc content. By contrast, at high concentrations of dietary zinc, worms are in a physiological state that minimizes uptake of dietary zinc and/or maximizes zinc excretion, so that animals respond to an increase in dietary zinc with a minimal increase in zinc content. Because zinc content never appears to be independent of dietary zinc, even at toxic levels of dietary zinc, it appears that worms do not have the capacity to maintain a consistent zinc content when challenged with increasing dietary zinc. These results support the model that excess zinc content is the cause of dietary zinc toxicity.

The analysis of metal content of worms indicated that there is a relationship between zinc metabolism and the metabolism of other metals, specifically copper and manganese. Wild-type worms displayed approximately twofold decreases in copper and manganese content as dietary zinc was increased. Interestingly, this effect was abrogated in *cdf-1* mutants. In humans, excess dietary zinc can cause copper deficiency (Prasad *et al.* 1978; Vallee and Falchuk 1993). Although the mechanisms have not been well established, one possibility is that processes that are regulated to excrete excess zinc and/or limit zinc uptake also act on other metals such as copper, perhaps due to overlapping specificity. Our results suggest that similar events occur in *C. elegans* and raise the possibility that mechanisms that promote zinc excretion or limit zinc uptake may also act on copper and manganese.

Studies of zinc in widely divergent species have led to the proposal that these systems have similar concentrations of zinc and that there is a universal zinc quotient (Outten and O'halloran 2001; Eide 2006). The results of our studies indicate that zinc content is dependent upon the concentration of dietary zinc and, therefore, highly variable. These findings suggest that animals have a measurable but limited capacity to moderate changes in zinc content in response to changing dietary zinc and probably have also evolved mechanisms to cope with a wide range of zinc content. Our studies measured total zinc content of the animals, and it is possible that the distribution of zinc within the animal is dynamic so that some cells or compartments maintain a relatively constant zinc concentration. For example, zinc may be sequestered in specific cells or compartments under conditions of high dietary zinc. Our analysis of *cdf-2* suggests that zinc is stored in vesicles of intestinal cells. The development of methods to localize zinc will be important for elucidating how worms partition zinc to different compartments, which may be an important aspect of zinc homeostasis.

***cdf-2* encodes a predicted zinc transporter that is localized to vesicles in intestinal cells:** We investigated *cdf-2* because it is predicted to encode a highly conserved member of the CDF family that is most similar to vertebrate ZnT-2 and is highly related to ZnT-3, ZnT-4, and ZnT-8. ZnT-2 is expressed in the small intestine, kidney, seminal vesicle, testis, and prostate and localized to the endosomal compartment (Palmiter *et al.* 1996a). ZnT-4 is expressed ubiquitously and localized to the *trans*-golgi network and endosomal compartment (Murgia *et al.* 1999). ZnT-3 is expressed in neurons and localized to synaptic vesicles (Palmiter *et al.* 1996b), and ZnT-8 is expressed in the pancreas and localized to insulin-containing vesicles (Chimienti *et al.* 2004, 2006). We used a CDF-2::GFP fusion protein to demonstrate that CDF-2 is localized to vesicles of intestinal cells. The vesicles that contain CDF-2::GFP colocalize with autofluorescent intestinal granules. Autofluorescent intestinal granules have been characterized by electron microscopy, leading to the conclusion that these structures are secondary lysosomes (Clokey and Jacobson 1986). Furthermore, autofluorescent intestinal granules colocalize with LysoTracker Red-stained compartments and acidified, acridine orange-stained compartments, strongly suggesting that these granules are components of lysosome-related organelles (Hermann *et al.* 2005). In light of these studies, our results indicate that CDF-2 resides on the membrane of secondary lysosomes/lysosome-related organelles. Thus, CDF-2 resembles ZnT-3 and ZnT-8 since it is expressed in a specific tissue and localized to specialized vesicles.

The discovery that CDF-2 is localized to lysosome-related organelles raises the interesting question: What is the role of zinc in the lumen of this compartment? *cdf-2* loss-of-function mutations caused impaired growth, indicating that the function of CDF-2 in lysosome-

related organelles is critical for optimal zinc metabolism and growth. The *cdf-2* mRNA was significantly increased by high dietary zinc, indicating that *cdf-2* may mediate a response to zinc stress. Taubert *et al.* (2008) analyzed the MDT-15 transcriptional coregulator and showed that the increase in *cdf-2* transcripts requires MDT-15. In conditions of high dietary zinc, CDF-2 may function to reduce cytosolic levels of zinc by sequestration in the lumen of lysosome-related organelles. Consistent with this possibility, *cdf-2* mRNA is induced by high dietary zinc and *cdf-2* mutant animals have reduced zinc content at high dietary zinc, suggestive of a storage defect. Strikingly, the zinc content of *cdf-2* mutant animals is one-third the zinc content of wild-type animals at high dietary zinc, suggesting that two-thirds of the zinc content of wild-type animals is stored in the lumen of intestinal vesicles. Another possibility is that CDF-2 functions to provide zinc for lysosomal enzymes. There are precedents for metal transporters supplying proteins resident in vesicles, such as the recent demonstration that ATP7A supplies copper to tyrosinase by functioning within specialized organelles called melanosomes (Setty *et al.* 2008). The yeast CDF proteins Msc2 and Zrg17 transport zinc into the ER to supply zinc to proteins in the secretory pathway (Ellis *et al.* 2005; Eide 2006), and vertebrate ZnT-3 and ZnT-8 transport zinc into synaptic vesicles and insulin-containing vesicles, respectively (Palmiter and Huang 2004). Our studies lay the foundation for further testing these hypotheses directly by establishing a model system to study the function of a CDF protein that is localized to the vesicular membrane.

***cdf-1* and *cdf-2* function antagonistically to regulate zinc metabolism:** Animals such as *C. elegans* and vertebrates contain extensive families of CDF proteins (Kambe *et al.* 2004; Liuzzi and Cousins 2004; Palmiter and Huang 2004; Eide 2006). It is important to determine the extent to which these proteins have independent, redundant, or antagonistic functions. In vertebrates, loss-of-function mutations have been described for ZnT-1, ZnT-3, ZnT-4, and ZnT-5 (Palmiter and Huang 2004); only ZnT-1 is essential for survival (Andrews *et al.* 2004). However, mutant animals that lack the function of two or more vertebrate *cdf* genes have not been reported.

Three *C. elegans* genes encoding cation diffusion facilitator proteins have now been characterized genetically and molecularly—*cdf-1*, *cdf-2*, and *sur-7*. *cdf-1* encodes a protein whose most similar vertebrate homolog is ZnT-1. CDF-1 and ZnT-1 are localized to the plasma membrane, ZnT-1 can functionally substitute for CDF-1 in *C. elegans*, and both proteins modulate Ras-mediated signaling in vertebrates and *C. elegans* (Bruinsma *et al.* 2002). *cdf-1* is expressed in vulval precursor cells, and it appears to act cell autonomously in these cells to affect Ras-mediated signaling. *cdf-1* is also highly expressed in intestinal cells, and *cdf-1* appears to act nonautonomously

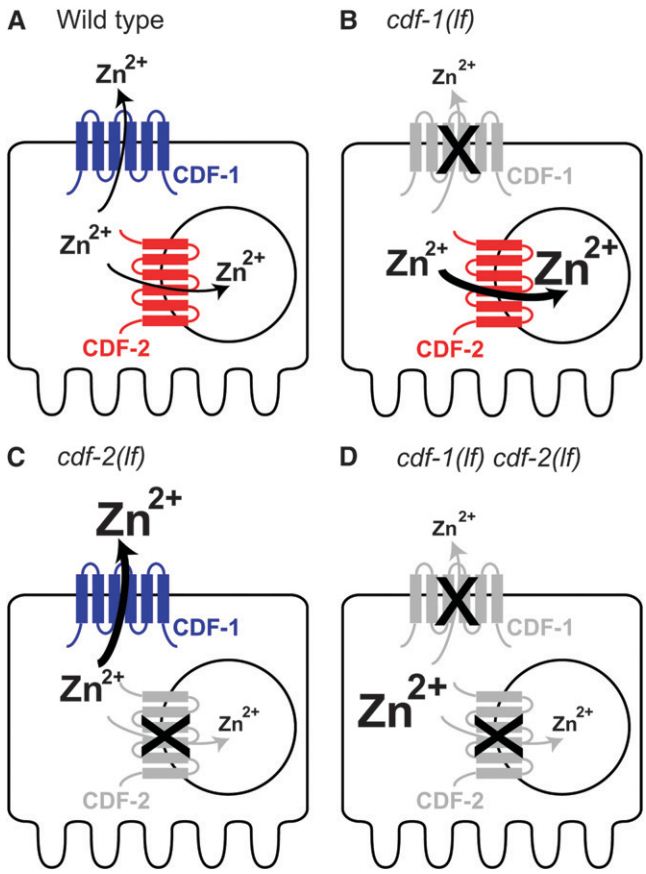

Figure 10.—A model of zinc distribution in wild-type and *cdf* mutant animals. Each diagram shows a polarized intestinal cell. CDF-1 (blue) localizes to the plasma membrane, and CDF-2 (red) localizes to the membrane of an intracellular compartment. The absence of CDF-1 and CDF-2 in mutant animals is illustrated by an X (B–D). The size of the Zn^{2+} indicates the concentration of zinc in a compartment. We propose that CDF-1 and CDF-2 function as zinc transporters on the basis of sequence similarity to well-characterized CDF proteins, and the size of the arrow indicates the amount of zinc flux. (A) In wild-type animals, CDF-1 and CDF-2 compete for cytosolic zinc, resulting in intermediate levels of zinc in the cytosol, the extracellular space, and the vesicle lumen. (B) In *cdf-1(lf)* mutant animals, the level of cytosolic zinc increases, and CDF-2 transports additional zinc into the vesicle lumen. (C) In *cdf-2(lf)* mutant animals, the level of cytosolic zinc increases, and CDF-1 transports additional zinc into the extracellular space. (D) In *cdf-1(lf) cdf-2(lf)* double mutant animals, zinc transport into both the vesicle lumen and extracellular space decreases.

in intestinal cells to affect Ras-mediated signaling in vulval precursor cells. CDF-1 may transport zinc from intestinal cells to the body cavity or intestinal lumen and thereby influence zinc metabolism in vulval precursor cells. A *cdf-1(lf)* mutant was previously demonstrated to be hypersensitive to high dietary zinc (Bruinsma *et al.* 2002). Here we confirmed this result using fully defined CeMM. We determined that the maturation of a *cdf-1(lf)* mutant was normal at optimal levels of dietary zinc but sensitive to low and high dietary zinc. The population growth rate of *cdf-1(lf)* mutant animals was reduced at all

concentrations of dietary zinc, but the mutant animals were extremely sensitive to high dietary zinc. *cdf-1(lf)* mutant animals displayed increased zinc content that was most pronounced at high levels of dietary zinc. These results indicate that *cdf-1* activity promotes zinc excretion and/or limits zinc uptake. One model to explain this observation is that CDF-1 transports zinc across the plasma membrane of intestinal cells and into the intestinal lumen, thus directly promoting zinc excretion. Alternatively, CDF-1 may transport zinc from intestinal cells into the body cavity, thereby indirectly promoting zinc excretion by another cell such as the excretory cell. The findings that *cdf-1* mutant animals cultured with high dietary zinc displayed increased zinc content and decreased survival suggest that the increased zinc content may cause the reduced survival.

sur-7 encodes a CDF protein that does not have a closely related homolog in vertebrates. Yoder *et al.* (2004) reported that a SUR-7::GFP fusion protein was expressed in nonintestinal cells in a cytosolic pattern suggestive of endoplasmic reticulum, indicating that *sur-7* may provide zinc to proteins resident in this compartment and promote excretion of zinc from cells through the secretory pathway. Here we demonstrated that *sur-7(lf)* mutant animals displayed reduced maturation and population growth rates in high dietary zinc, consistent with previous reports (Yoder *et al.* 2004). Maturation was also reduced at low dietary zinc, whereas mutant and wild-type animals displayed similar maturation at a narrow range of optimal dietary zinc. The zinc content of *sur-7* mutant animals was similar to wild-type animals. Because the growth defects of *sur-7* mutants are evidence for altered zinc metabolism, the finding that the overall zinc content is similar to wild type indicates that the distribution of zinc in the *sur-7(lf)* mutant animals is abnormal. The *sur-7* phenotypes may be caused by reduced zinc in the secretory pathway and/or increased zinc in another compartment.

Because CDF-1, CDF-2, and SUR-7 are all predicted to reduce the concentration of zinc in the cytoplasm, it is possible that the functions of these proteins are redundant. In this case, double or triple mutant animals might display phenotypes that are stronger than any single mutant. In general, we did not observe this pattern, since most double and triple mutant animals displayed similar phenotypes to one of the single mutants. However, for the phenotype of controlling zinc content in high dietary zinc (Figure 9H), the triple mutant was much more impaired than any single mutant. This result suggests that CDF-1, CDF-2, and SUR-7 might function redundantly to control zinc content at high dietary zinc.

By contrast to the similar effects that all CDF proteins are predicted to have on the cytoplasmic zinc concentration, CDF-1 and CDF-2 are predicted to have distinct effects on zinc concentrations in the extracellular space and lumen of intracellular compartments. Whereas *cdf-1(lf)* mutant animals displayed increased zinc content in high dietary zinc, suggesting *cdf-1* is necessary to excrete zinc, *cdf-2(lf)* mutant animals displayed reduced zinc content in high dietary zinc, suggesting *cdf-2* is necessary to store zinc. The *cdf-1 cdf-2* double mutant displayed an intermediate zinc content, suggesting that *cdf-1* and *cdf-2* function antagonistically. CDF-1 and CDF-2 are both expressed in intestinal cells; CDF-1 is localized to the plasma membrane, whereas CDF-2 is localized to vesicles. As shown in Figure 10, we propose that CDF-1 and CDF-2 compete for cytosolic zinc. If CDF-1 transports zinc across the plasma membrane, then the zinc content of the animal is directly or indirectly decreased. If CDF-2 transports zinc into the vesicle lumen, then the zinc content of the animal is increased. This model accounts for the changes observed in the *cdf-1* and *cdf-2* mutant animals and explains why the *cdf-1 cdf-2* double mutant animals have an intermediate phenotype. These findings demonstrate the power of the *C. elegans* model system to dissect the relationships between CDF family members.

Some strains were provided by the Caenorhabditis Genetics Center. We are grateful to Shohei Mitani for providing the *cdf-2(tm788)* allele, Min Han for providing the *sur-7(ku119)* allele, Andrew Fire for providing the pRF4 and pPD95.77 plasmids, Judith Austin for providing the pMM016 plasmid, Sudhir Nayak for assistance with biolistic bombardment, Shin-ichiro Imai for use of the spectrophotometer, Irving Boime for helpful discussions, Danielle Pepin for generating the pDG222 and pDP15 plasmids, Ivan Dimitrov for cDNA preparation, and Christopher Pickett for help in immunostaining. This research was supported by grants from the National Institutes of Health to K.K. (GM068598, AC84271, and AG026561). K.K. is a senior scholar of the Ellison Medical Foundation.

LITERATURE CITED

Andrews, G. K., H. Wang, S. K. Dey and R. D. Palmiter, 2004 Mouse zinc transporter 1 gene provides an essential function during early embryonic development. Genesis **40:** 74–81.

Beitel, G. J., S. G. Clark and H. R. Horvitz, 1990 *Caenorhabditis elegans* ras gene *let-60* acts as a switch in the pathway of vulval induction. Nature **348:** 503–509.

Brenner, S., 1974 The genetics of *Caenorhabditis elegans*. Genetics **77:** 71–94.

Bruinsma, J. J., T. Jirakulaporn, A. J. Muslin and K. Kornfeld, 2002 Zinc ions and cation diffusion facilitator proteins regulate Ras-mediated signaling. Dev. Cell **2:** 567–578.

Bruinsma, J. J., D. L. Schneider, D. E. Davis and K. Kornfeld, 2008 Identification of mutations in *Caenorhabditis elegans* that cause resistance to high levels of dietary zinc and analysis using a genomewide map of single nucleotide polymorphisms scored by pyrosequencing. Genetics **179:** 811–828.

Buecher, Jr., E. J., E. Hansen and E. A. Yarwood, 1966 Ficoll activation of a protein essential for maturation of the free-living nematode *Caenorhabditis briggsae*. Proc. Soc. Exp. Biol. Med. **121:** 390–393.

Chao, Y., and D. Fu, 2004 Kinetic study of the antiport mechanism of an *Escherichia coli* zinc transporter, ZitB. J. Biol. Chem. **279:** 12043–12050.

Chimienti, F., S. Devergnas, A. Favier and M. Seve, 2004 Identification and cloning of a beta-cell-specific zinc transporter, ZnT-8, localized into insulin secretory granules. Diabetes **53:** 2330–2337.

Chimienti, F., S. Devergnas, F. Pattou, F. Schuit, R. Garcia-Cuenca *et al.*, 2006 *In vivo* expression and functional characterization

of the zinc transporter ZnT8 in glucose-induced insulin secretion. J. Cell Sci. **119:** 4199–4206.

Chowanadisai, W., S. L. Kelleher and B. Lonnerdal, 2005 Zinc deficiency is associated with increased brain zinc import and LIV-1 expression and decreased ZnT-1 expression in neonatal rats. J. Nutr. **135:** 1002–1007.

Chowanadisai, W., B. Lonnerdal and S. L. Kelleher, 2006 Identification of a mutation in SLC30A2 (ZnT-2) in women with low milk zinc concentration that results in transient neonatal zinc deficiency. J. Biol. Chem. **281:** 39699–39707.

Clokey, G. V., and L. A. Jacobson, 1986 The autofluorescent "lipofuscin granules" in the intestinal cells of *Caenorhabditis elegans* are secondary lysosomes. Mech. Ageing Dev. **35:** 79–94.

Cole, T. B., H. J. Wenzel, K. E. Kafer, P. A. Schwartzkroin and R. D. Palmiter, 1999 Elimination of zinc from synaptic vesicles in the intact mouse brain by disruption of the ZnT3 gene. Proc. Natl. Acad. Sci. USA **96:** 1716–1721.

Dong, J., W. A. Boyd and J. H. Freedman, 2008a Molecular characterization of two homologs of the *Caenorhabditis elegans* cadmium-responsive gene *cdr-1*: *cdr-4* and *cdr-6*. J. Mol. Biol. **376:** 621–633.

Dong, J., J. D. Robertson, W. R. Markesbery and M. A. Lovell, 2008b Serum zinc in the progression of Alzheimer's disease. J. Alzheimers Dis. **15:** 443–450.

Duerr, J. S., 2006 Immunohistochemistry (June 19, 2006), *WormBook*, ed. The *C. elegans* Research Community, WormBook, doi/10.1895/wormbook.1.105.1, http://www.wormbook.org.

Dufner-Beattie, J., B. P. Weaver, J. Geiser, M. Bilgen, M. Larson *et al.*, 2007 The mouse acrodermatitis enteropathica gene Slc39a4 (Zip4) is essential for early development and heterozygosity causes hypersensitivity to zinc deficiency. Hum. Mol. Genet. **16:** 1391–1399.

Eide, D. J., 2004 The SLC39 family of metal ion transporters. Pflugers Arch. **447:** 796–800.

Eide, D. J., 2006 Zinc transporters and the cellular trafficking of zinc. Biochim. Biophys. Acta **1763:** 711–722.

Ellis, C. D., C. W. Macdiarmid and D. J. Eide, 2005 Heteromeric protein complexes mediate zinc transport into the secretory pathway of eukaryotic cells. J. Biol. Chem. **280:** 28811–28818.

Eng, B. H., M. L. Guerinot, D. Eide and M. H. Saier, Jr., 1998 Sequence analyses and phylogenetic characterization of the ZIP family of metal ion transport proteins. J. Membr. Biol. **166:** 1–7.

Gaither, L. A., and D. J. Eide, 2001 Eukaryotic zinc transporters and their regulation. Biometals **14:** 251–270.

Guerinot, M. L., 2000 The ZIP family of metal transporters. Biochim. Biophys. Acta **1465:** 190–198.

Guffanti, A. A., Y. Wei, S. V. Rood and T. A. Krulwich, 2002 An antiport mechanism for a member of the cation diffusion facilitator family: divalent cations efflux in exchange for K+ and H+. Mol. Microbiol. **45:** 145–153.

Hambidge, K. M., and N. F. Krebs, 2007 Zinc deficiency: a special challenge. J. Nutr. **137:** 1101–1105.

Hambidge, M., 2000 Human zinc deficiency. J. Nutr. **130:** 1344S–1349S.

Herbig, A., A. J. Bird, S. Swierczek, K. McCall, M. Mooney *et al.*, 2005 Zap1 activation domain 1 and its role in controlling gene expression in response to cellular zinc status. Mol. Microbiol. **57:** 834–846.

Hermann, G. J., L. K. Schroeder, C. A. Hieb, A. M. Kershner, B. M. Rabbitts *et al.*, 2005 Genetic analysis of lysosomal trafficking in *Caenorhabditis elegans*. Mol. Biol. Cell. **16:** 3273–3288.

Hieb, W. F., and M. Rothstein, 1968 Sterol requirement for reproduction of a free-living nematode. Science **160:** 778–780.

Hieb, W. F., E. L. Stokstad and M. Rothstein, 1970 Heme requirement for reproduction of a free-living nematode. Science **168:** 143–144.

Horvitz, H. R., M. Chalfie, C. Trent, J. E. Sulston and P. D. Evans, 1982 Serotonin and octopamine in the nematode *Caenorhabditis elegans*. Science **216:** 1012–1014.

Kambe, T., Y. Yamaguchi-Iwai, R. Sasaki and M. Nagao, 2004 Overview of mammalian zinc transporters. Cell. Mol. Life Sci. **61:** 49–68.

Kemp, B. J., D. L. Church, J. Hatzold, B. Conradt and E. J. Lambie, 2009 *gem-1* encodes an SLC16 monocarboxylate transporter-related protein that functions in parallel to the *gon-2* TRPM channel during gonad development in *Caenorhabditis elegans*. Genetics **181:** 581–591.

Koh, J. Y., S. W. Suh, B. J. Gwag, Y. Y. He, C. Y. Hsu *et al.*, 1996 The role of zinc in selective neuronal death after transient global cerebral ischemia. Science **272:** 1013–1016.

Liuzzi, J. P., and R. J. Cousins, 2004 Mammalian zinc transporters. Annu. Rev. Nutr. **24:** 151–172.

Lu, M., and D. Fu, 2007 Structure of the zinc transporter YiiP. Science **317:** 1746–1748.

Lu, N. C., and K. M. Goetsch, 1993 Carbohydrate requirement of *Caenorhabditis elegans* and the final development of a chemically defined medium. Nematologica **39:** 303–311.

Lu, N. C., G. Hugenberg, G. M. Briggs and E. L. Stokstad, 1978 The growth-promoting activity of several lipid-related compounds in the free-living nematode *Caenorhabditis briggsae*. Proc. Soc. Exp. Biol. Med. **158:** 187–191.

Maduro, M., and D. Pilgrim, 1995 Identification and cloning of *unc-119*, a gene expressed in the *Caenorhabditis elegans* nervous system. Genetics **141:** 977–988.

Maverakis, E., M. A. Fung, P. J. Lynch, M. Draznin, D. J. Michael *et al.*, 2007 Acrodermatitis enteropathica and an overview of zinc metabolism. J. Am. Acad. Dermatol. **56:** 116–124.

Mello, C. C., J. M. Kramer, D. Stinchcomb and V. Ambros, 1991 Efficient gene transfer in *C. elegans*: extrachromosomal maintenance and integration of transforming sequences. EMBO J. **10:** 3959–3970.

Murgia, C., I. Vespignani, J. Cerase, F. Nobili and G. Perozzi, 1999 Cloning, expression, and vesicular localization of zinc transporter Dri 27/ZnT4 in intestinal tissue and cells. Am. J. Physiol. **277:** G1231–G1239.

Nies, D. H., 2007 Biochemistry. How cells control zinc homeostasis. Science **317:** 1695–1696.

Outten, C. E., and T. V. O'Halloran, 2001 Femtomolar sensitivity of metalloregulatory proteins controlling zinc homeostasis. Science **292:** 2488–2492.

Palmiter, R. D., and S. D. Findley, 1995 Cloning and functional characterization of a mammalian zinc transporter that confers resistance to zinc. EMBO J. **14:** 639–649.

Palmiter, R. D., T. B. Cole and S. D. Findley, 1996a ZnT-2, a mammalian protein that confers resistance to zinc by facilitating vesicular sequestration. EMBO J. **15:** 1784–1791.

Palmiter, R. D., T. B. Cole, C. J. Quaife and S. D. Findley, 1996b ZnT-3, a putative transporter of zinc into synaptic vesicles. Proc. Natl. Acad. Sci. USA **93:** 14934–14939.

Palmiter, R. D., and L. Huang, 2004 Efflux and compartmentalization of zinc by members of the SLC30 family of solute carriers. Pflugers Arch. **447:** 744–751.

Pfaffl, M. W., 2001 A new mathematical model for relative quantification in real-time RT-PCR. Nucleic Acids Res. **29:** e45.

Praitis, V., E. Casey, D. Collar and J. Austin, 2001 Creation of low-copy integrated transgenic lines in *Caenorhabditis elegans*. Genetics **157:** 1217–1226.

Prasad, A. S., G. J. Brewer, E. B. Schoomaker and P. Rabbani, 1978 Hypocupremia induced by zinc therapy in adults. J. Am. Med. Assoc. **240:** 2166–2168.

Pulak, R., 2006 Techniques for analysis, sorting, and dispensing of *C. elegans* on the COPAS flow-sorting system. Methods Mol. Biol. **351:** 275–286.

Rajagopal, A., A. U. Rao, J. Amigo, M. Tian, S. K. Upadhyay *et al.*, 2008 Haem homeostasis is regulated by the conserved and concerted functions of HRG-1 proteins. Nature **453:** 1127–1131.

Riddle, D. L., T. Blumental, B. J. Meyer and J. R. Preiss, 1997 *C. elegans II*. Cold Spring Harbor Laboratory Press, Cold Spring Harbor, NY.

Setty, S. R., D. Tenza, E. V. Sviderskaya, D. C. Bennett, G. Raposo *et al.*, 2008 Cell-specific ATP7A transport sustains copper-dependent tyrosinase activity in melanosomes. Nature **454:** 1142–1146.

Seve, M., F. Chimienti, S. Devergnas and A. Favier, 2004 *In silico* identification and expression of SLC30 family genes: an expressed sequence tag data mining strategy for the characterization of zinc transporters' tissue expression. BMC Genomics **5:** 32.

Stryer, L., 1995 *Biochemistry*. W. H. Freeman, New York.

Szewczyk, N. J., E. Kozak and C. A. Conley, 2003 Chemically defined medium and *Caenorhabditis elegans*. BMC Biotechnol. **3:** 19.

Szewczyk, N. J., I. A. Udranszky, E. Kozak, J. Sunga, S. K. Kim *et al.*, 2006 Delayed development and lifespan extension as features of metabolic lifestyle alteration in *C. elegans* under dietary restriction. J. Exp. Biol. **209:** 4129–4139.

Tapiero, H., and K. D. Tew, 2003 Trace elements in human physiology and pathology: zinc and metallothioneins. Biomed. Pharmacother. **57:** 399–411.

Taubert, S., M. Hansen, M. R. Van Gilst, S. B. Cooper and K. R. Yamamoto, 2008 The Mediator subunit MDT-15 confers metabolic adaptation to ingested material. PLoS Genet. **4:** e1000021.

Vallee, B. L., and K. H. Falchuk, 1993 The biochemical basis of zinc physiology. Physiol. Rev. **73:** 79–118.

Vandesompele, J., K. De Preter, F. Pattyn, B. Poppe, N. Van Roy *et al.*, 2002 Accurate normalization of real-time quantitative RT-PCR data by geometric averaging of multiple internal control genes. Genome Biol. **3:** RESEARCH0034.

Wood, W. B., 1988 *The Nematode Caenorhabditis elegans*. Cold Spring Harbor Laboratory Press, Cold Spring Harbor, NY.

Yoder, J. H., H. Chong, K. L. Guan and M. Han, 2004 Modulation of KSR activity in *Caenorhabditis elegans* by Zn ions, PAR-1 kinase and PP2A phosphatase. EMBO J. **23:** 111–119.

Zhao, H., and D. J. Eide, 1997 Zap1p, a metalloregulatory protein involved in zinc-responsive transcriptional regulation in *Saccharomyces cerevisiae*. Mol. Cell. Biol. **17:** 5044–5052.

Communicating editor: B. J. Meyer

GENETICS

Supporting Information
http://www.genetics.org/cgi/content/full/genetics.109.103614/DC1

The Cation Diffusion Facilitator Gene *cdf-2* Mediates Zinc Metabolism in *Caenorhabditis elegans*

Diana E. Davis, Hyun Cheol Roh, Krupa Deshmukh, Janelle J. Bruinsma, Daniel L. Schneider, James Guthrie, J. David Robertson and Kerry Kornfeld

DOI: 10.1534/genetics.109.103614

TABLE S1

Metal content of wild-type and mutant *C. elegans* determined by ICP-MS

Metal	Genotype[a]	Dietary Zinc (μM) 6	10	30	75	350	1000	2000
Zinc	WT	37	50	79	135	306	550	1003
	cdf-1	33	51	107	160	344	792	1532
	cdf-2	37	41	50	72	111	199	357
	sur-7	43	59	104	153	311	619	1114
	cdf-1 cdf-2	33	43	56	70	130	374	779
	cdf-1 sur-7	34	44	87	144	345	901	1637
	cdf-1 cdf-2 sur-7	32	40	58	70	153	444	1046
Copper	WT	192	197	177	174	142	124	114
	cdf-1	167	200	195	172	127	142	176
	cdf-2	191	168	169	162	142	163	143
	sur-7	174	174	158	153	137	111	99
	cdf-1 cdf-2	166	156	142	141	138	168	177
	cdf-1 sur-7	178	157	155	155	137	144	183
	cdf-1 cdf-2 sur-7	183	171	166	138	143	179	173
Iron	WT	154	166	123	135	111	132	146
	cdf-1	187	180	173	155	151	172	239
	cdf-2	130	122	121	159	125	149	114
	sur-7	133	134	127	128	127	121	138
	cdf-1 cdf-2	170	168	152	148	152	178	219
	cdf-1 sur-7	204	178	162	173	150	186	213
	cdf-1 cdf-2 sur-7	201	205	194	159	196	219	237
Manganese	WT	341	304	329	313	237	223	218
	cdf-1	398	410	376	318	262	283	360
	cdf-2	502	459	465	348	319	397	315
	sur-7	415	399	343	315	244	249	238
	cdf-1 cdf-2	427	403	338	330	318	360	423
	cdf-1 sur-7	445	381	344	300	292	356	397
	cdf-1 cdf-2 sur-7	496	463	422	352	362	490	492

Values are the metal content in parts per million by weight.

[a] Mutant alleles were *cdf-1(n2527)*, *cdf-2(tm788)*, and *sur-7(ku119)*.

TABLE S2

Maturation of *C. elegans* determined by COPAS BIOSORT

	Genotype[a]							
Dietary zinc (μM)	WT	*cdf-1*	*cdf-2*	*sur-7*	*cdf-1 cdf-2*	*cdf-2 sur-7*	*cdf-1 sur-7*	*cdf-1 cdf-2 sur-7*
0	129 ± 6	113 ± 2	125 ± 3	99 ± 11	101 ± 4	88 ± 2	99 ± 6	93 ± 3
1	141 ± 3	118 ± 3	136 ± 7	99 ± 4	97 ± 3	91 ± 1	103 ± 5	89 ± 3
2	140 ± 6	119 ± 6	136 ± 1	103 ± 1	102 ± 4	98 ± 7	99 ± 2	91 ± 4
4	151 ± 5	122 ± 5	145 ± 8	110 ± 2	107 ± 4	95 ± 1	102 ± 4	98 ± 6
6	154 ± 5	122 ± 7	153 ± 8	120 ± 4	112 ± 4	103 ± 3	102 ± 8	101 ± 3
8	158 ± 2	135 ± 12	154 ± 4	126 ± 7	118 ± 4	104 ± 2	109 ± 6	107 ± 8
10	166 ± 7	152 ± 2	156 ± 5	137 ± 5	125 ± 21	137 ± 7	110 ± 7	117 ± 10
20	173 ± 12	166 ± 3	167 ± 11	147 ± 3	144 ± 8	148 ± 2	111 ± 4	139 ± 10
30	171 ± 4	167 ± 8	174 ± 2	156 ± 6	145 ± 9	152 ± 7	114 ± 6	148 ± 7
40	164 ± 2	183 ± 11	171 ± 3	153 ± 11	147 ± 7	149 ± 3	120 ± 6	156 ± 16
50	170 ± 5	181 ± 11	172 ± 1	152 ± 7	147 ± 8	154 ± 7	117 ± 7	153 ± 5
60	173 ± 6	182 ± 17	173 ± 7	159 ± 6	143 ± 5	149 ± 6	110 ± 6	144 ± 10
150	173 ± 0.3	136 ± 8	167 ± 7	137 ± 5	117 ± 12	139 ± 7	112 ± 6	136 ± 6
300	170 ± 4	129 ± 20	162 ± 9	115 ± 1	95 ± 10	113 ± 6	101 ± 6	136 ± 6
400	169 ± 4	117 ± 7	161 ± 2	106 ± 5	97 ± 7	108 ± 4	99 ± 3	106 ± 4
600	161 ± 8	106 ± 6	151 ± 13	100 ± 4	95 ± 2	101 ± 3	95 ± 3	100 ± 2
800	161 ± 9	104 ± 4	152 ± 6	102 ± 3	94 ± 5	99 ± 5	96 ± 2	93 ± 3
1000	158 ± 9	108 ± 8	147 ± 8	102 ± 3	90 ± 6	94 ± 1	NA	95 ± 3

Values are the average time of flight (±SD) of four biological replicates.

[a] Mutant alleles were *cdf-1(n2527)*, *cdf-2(tm788)*, and *sur-7(ku119)*.

TABLE S3

Population growth rate of wild-type and mutant *C. elegans*

	Genotype[a]							
Dietary zinc (μM)	WT	*cdf-1*	*cdf-2*	*sur-7*	*cdf-1 cdf-2*	*cdf-2 sur-7*	*cdf-1 sur-7*	*cdf-1 cdf-2 sur-7*
0	1 ± 1	0.5 ± 0.3	0.1 ± 0.1	0.4 ± 0.1	0.1 ± 0.2	0.2 ± 0.2	0.7 ± 0.9	0.0 ± 0.2
1	1 ± 1	0.5 ± 0.7	-0.05 ± 0.4	0.7 ± 0.3	0.3 ± 0.4	0.51 ± 0.01	0.7 ± 0.6	0.2 ± 0.1
2	3 ± 1	0.9 ± 0.7	1.9 ± 0.9	1.4 ± 0.2	0.5 ± 0.8	0.5 ± 0.3	1 ± 1	0.44 ± 0.03
4	9 ± 4	1.4 ± 0.8	8 ± 5	3.5 ± 0.8	2 ± 2	2.0 ± 0.02	3 ± 3	2 ± 1
6	12 ± 4	3 ± 1	15 ± 7	6 ± 3	4 ± 3	3.9 ± 0.8	5 ± 2	4.1 ± 0.9
8	16 ± 6	3.2 ± 0.5	18 ± 4	8 ± 1	7 ± 7	5 ± 0	8 ± 4	5 ± 3
10	22 ± 5	5 ± 5	17 ± 3	7 ± 3	9 ± 7	7 ± 1	16 ± 1	9 ± 1
15	30 ± 8	5 ± 4	13 ± 3	7 ± 3	11 ± 10	8 ± 3	20 ± 0	11 ± 2
30	31 ± 7	6 ± 5	11 ± 1	7 ± 5	9 ± 6	9 ± 1	19 ± 1	12 ± 3
60	26 ± 8	3.4 ± 0.9	12.0 ± 0.7	10 ± 4	5 ± 3	10 ± 3	14 ± 1	13 ± 3
120	24 ± 7	4 ± 1	15 ± 1	11 ± 4	7 ± 5	11 ± 2	14 ± 1	11 ± 3
240	23 ± 8	3 ± 2	15 ± 2	8 ± 2	5 ± 3	12 ± 1	12 ± 2	6 ± 2
480	22 ± 4	2 ± 2	14 ± 3	7 ± 2	3 ± 1	5 ± 2	8 ± 5	1.9 ± 0.2
960	16 ± 5	0.8 ± 0.7	15 ± 4	2 ± 1	0.9 ± 0.6	2.0 ± 0.2	3 ± 4	0.3 ± 0.4
1920	6 ± 2	0.6 ± 0.4	6 ± 2	0.1 ± 0.1	0.3 ± 0.4	0.5 ± 0.4	0.5 ± 0.8	0.0 ± 0.2
2500	3 ± 1	0.3 ± 0.2	4 ± 2	0.0 ± 0.1	0.3 ± 0.3	0.3 ± 0.4	0.5 ± 0.2	0.0 ± 0.2

Values are the average population growth rate (±SD) of 2-3 biological replicates (worms/mL/day x 1000).

[a] Mutant alleles were *cdf-1(n2527)*, *cdf-2(tm788)*, and *sur-7(ku119)*.

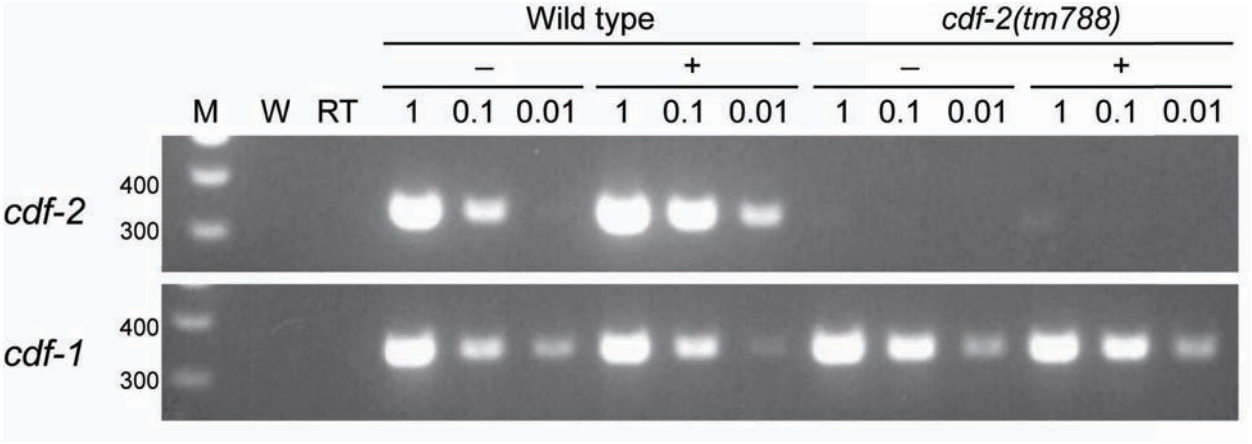

FIGURE S1.— *cdf-2* transcript levels were decreased ~1,000-fold in *cdf-2(tm788)* mutant animals. Mixed-stage wild-type and *cdf-2(tm788)* animals were cultured on NAMM dishes containing *E. coli* (BRUINSMA *et al.* 2008) and no supplemental zinc (-) or 0.5 mM supplemental zinc (+) for 40 hours at 20°. Animals were collected in M9 buffer and solubilized in TRIzol (Invitrogen). 590 ng of RNA was reverse transcribed using random hexamer primers and the SuperScript III First-Strand Synthesis System for RT-PCR (Invitrogen). cDNA was diluted in water and PCR amplified using KlenTaq LA DNA Polymerase (Sigma-Aldrich). The amount of input cDNA is indicated in arbitrary units (1, no dilution; 0.1, 10x dilution; 0.01, 100x dilution), and the intensity of the amplified products demonstrates the semi-quantitative nature of the assay. A 325 bp *cdf-2* product was amplified using primers that annealed to exon 5 and to the junction of exons 7 and 8. These exons are not affected by the *tm788* deletion. A 330 bp *cdf-1* product was amplified using primers that annealed to exons 3 and 4. As a control for contamination of individual reaction components, we substituted water for the templates and either PCR amplified (W) or reverse transcribed and PCR amplified (RT) the reaction mixes with each primer set. PCR products were separated on a 2% TAE agarose gel containing ethidium bromide and visualized using UV light. Molecular weight markers (M) are labeled (100 bp DNA ladder, New England Biolabs, Ipswich, MA). The identities of the amplified products were verified by DNA sequencing. In wild-type animals, *cdf-2* transcripts were readily detected and induced by supplemental zinc. In *cdf-2(tm788)* animals, *cdf-2* transcript levels were reduced ~1,000-fold compared to wild-type animals since they were barely detectable with 1 unit of input cDNA. Furthermore, *cdf-2* transcripts in the mutant animals were not induced by supplemental zinc. The *cdf-1* control demonstrates that equivalent levels of amplifiable cDNA were present in all of the samples.